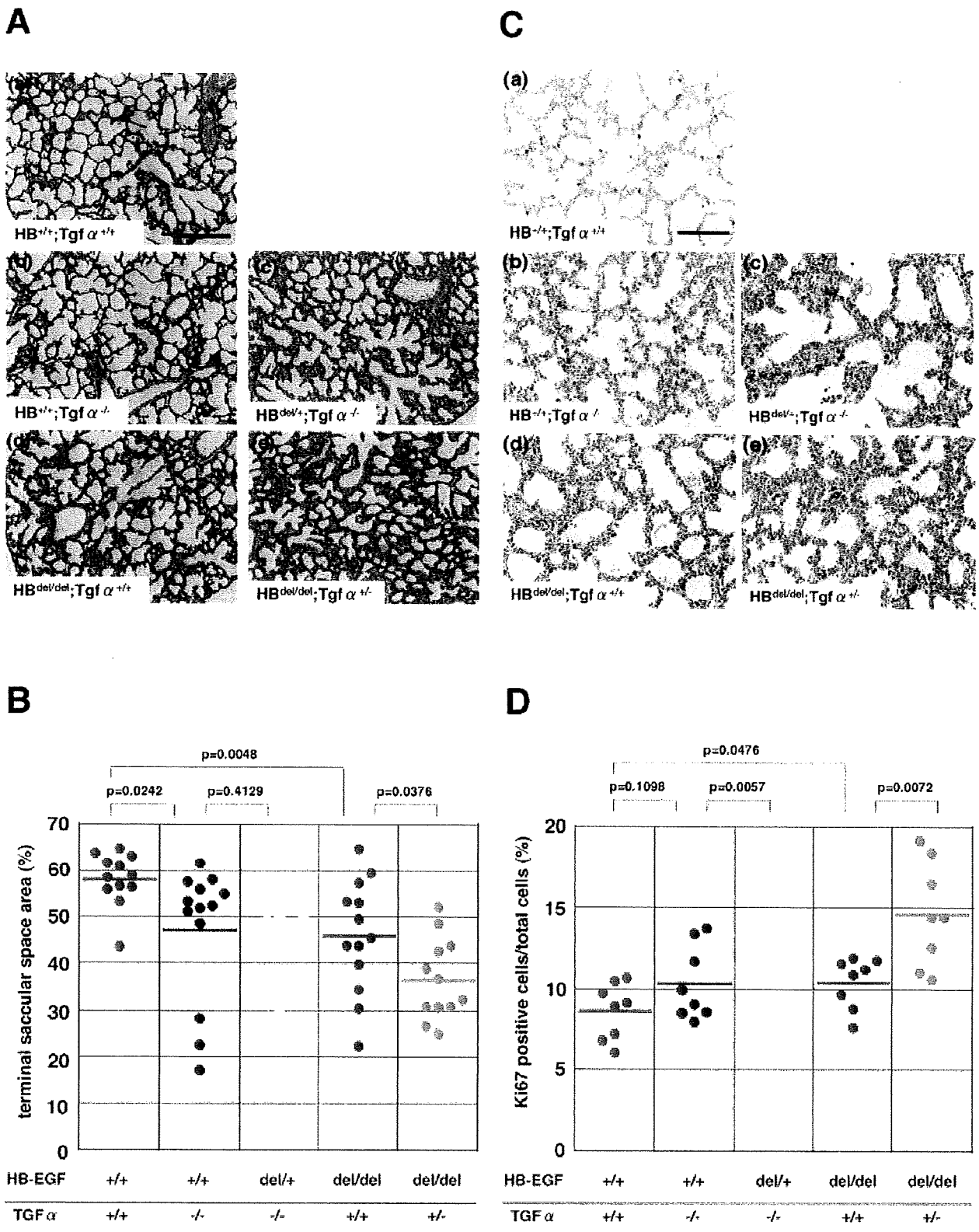
A
C
B
D
terminal saccular space area (%)
Ki67 positive cells/total cells (%)
p=0.0048
p=0.0242
p=0.4129
p=0.0376
p=0.0476
p=0.1098
p=0.0057
p=0.0072
HB-EGF
TGF α

Fig. 6.

that HB-EGF and TGFα function synergistically in perinatal distal lung formation.

## EGFR Is Involved in HB-EGF–Dependent Perinatal Distal Lung Development

EGFR is a receptor for both HB-EGF and TGFα (Harris et al., 2003) and is essential for normal lung development (Miettinen et al., 1995; Sibilia and Wagner, 1995). To determine whether EGFR acts as a receptor for HB-EGF in perinatal distal lung development, we used a hypomorphic EGFR mutant, waved 2, and tested for a genetic interaction with HB-EGF. In waved 2 mice, the kinase activity of EGFR is decreased to less than 10% that of wild-type EGFR, owing to a point mutation in the kinase domain (Luetteke et al., 1994; Fowler et al., 1995). Because intercrosses of $HB^{del/+}$; wa2/+ double-heterozygous male and female mice produced only 3 $HB^{del/del}$; wa2/wa2 double-homozygous newborn (in total 234 newborns from 36 litters), we statistically compared $HB^{del/del}$; wa2/+ and $HB^{del/+}$; wa2/wa2 lungs with $HB^{del/del}$; +/+ and $HB^{+/+}$; wa2/wa2 lungs, respectively, of newborns. Reduction of the TSSA in $HB^{+/+}$; wa2/wa2 single mutant compared with that in wild-type is significantly remarkable. Reduction of TSSA in $HB^{del/del}$; wa2/+ lungs was more frequent than that of $HB^{del/del}$; +/+, although not statistically significant (Fig. 7A,B). We could not detect remarkable differences in the other comparative combinations (Fig. 7A,B).

Regarding proliferation rates, the ratio of Ki67-positive cells to the total cells was significantly increased in $HB^{del/del}$; +/+ and $HB^{+/+}$; wa2/wa2 lungs compared with $HB^{+/+}$; +/+ wild-type lungs. A comparison of the ratio of Ki67-positive cells between $HB^{+/+}$; wa2/wa2 and $HB^{del/+}$; wa2/wa2 lungs showed no significant difference. On the other hand, $HB^{del/del}$; wa2/+ lungs showed a relatively higher ratio of Ki67-positive cells than $HB^{del/del}$; +/+ lungs, although not statistically significant (Fig. 7C,D). Although the statistical significance in this study was lower than those of the case of HB-EGF and TGFα double mutants, these results suggest that EGFR is involved in the inhibitory function of HB-EGF in perinatal distal lung development.

## DISCUSSION

We demonstrate here a novel role for HB-EGF in perinatal distal lung development. Our major findings are as follows: (1) HB-EGF is expressed in the lung epithelium and interstitium, and the mRNA level is gradually increased during the canalicular to perinatal saccular stage; (2) HB-EGF contributes to deceleration of perinatal cell proliferation in the distal lung; (3) HB-EGF functions synergistically with TGFα in this stage; (4) EGFR is involved in the HB-EGF function.

Although it has been previously reported that HB-EGF null newborns exhibit abnormal lung morphology (Jackson et al., 2003), the detailed information of such abnormality remains unclear. In this study, we demonstrate using HB-EGF null embryos and newborns that HB-EGF contributes to the deceleration of cell proliferation in the perinatal distal lung, based on the following findings: (1) $HB^{del/del}$ lungs showed significantly lower TSSA scores during perinatal saccular stage after E18.5 as compared to wild-type lungs; (2) in $HB^{del/del}$ lungs, the ratio of Ki67-positive cells in distal lungs was significantly higher than wild-type lungs in each stage examined; (3) only a few apoptotic cells were observed in the lungs in this stage, and no significant difference was detected between wild-type and $HB^{del/del}$ lungs. In this study, the possibility that HB-EGF is also involved in the lung inflation after birth cannot be ruled out; however, the major cause in the abnormally thick saccular walls in HB-EGF null lungs might be due to hypercellularity, because the rate of cell proliferation was significantly increased in the HB-EGF null lungs. Therefore, HB-EGF has an inhibitory function for cell proliferation in distal lungs during perinatal normal lung development. Consequently, the absence of HB-EGF resulted in the persistent deregulated hyperproliferative state in the distal lung cells. It is noteworthy that the ratio of Ki67-positive cells was decreased at birth even in $HB^{del/del}$ lungs, suggesting that there are some other factor(s) compensating HB-EGF functions, as discussed later.

HB-EGF has conventionally been thought of as a growth factor. Indeed, several lines of evidence point to a fundamental role for HB-EGF in cell proliferation and tumorigenesis (Miyamoto et al., 2006). However, no hypoplastic abnormalities have been found in HB-EGF null mice to date; rather, HB-EGF null mice exhibit hyperplastic abnormalities (Iwamoto et al., 2003; Jackson et al., 2003; Yamazaki et al., 2003; Iwamoto and Mekada, 2006) as well as defects in cell migration (Mine et al., 2005; Shirakata et al., 2005). These findings suggest that HB-EGF may not function as a growth factor in developmental and physiological processes. Importantly among these studies, the inhibitory function of HB-EGF for cell proliferation in vivo has also been reported in cardiac valve development (Iwamoto et al., 2003; Jackson et al., 2003; Yamazaki et al., 2003; Iwamoto and Mekada, 2006). In this process, HB-EGF is expressed only in the endocardial cells of developing cardiac valves, mainly during valve remodeling, and causes the inhibition of mesenchymal cell proliferation during valve remodeling. The molecular mechanisms that are involved in the inhibitory function of HB-EGF in both

**Fig. 6.** Comparison of TSSA and cell proliferation in double mutants of HB-EGF and TGFα newborn pups. **A:** Representative hematoxylin/eosin-stained sections of newborn lungs from $HB^{+/+}$;$Tgf\alpha^{+/+}$ (a), $HB^{+/+}$;$Tgf\alpha^{-/-}$ (b), $HB^{del/+}$;$Tgf\alpha^{-/-}$ (c), $HB^{del/del}$;$Tgf\alpha^{+/+}$ (d), and $HB^{del/del}$;$Tgf\alpha^{+/-}$ (e). **B:** Comparison of TSSA of newborn lungs from $HB^{+/+}$;$Tgf\alpha^{+/+}$, $HB^{+/+}$;$Tgf\alpha^{-/-}$, $HB^{del/+}$;$Tgf\alpha^{-/-}$, $HB^{del/del}$;$Tgf\alpha^{+/+}$, and $HB^{del/del}$;$Tgf\alpha^{+/-}$. Each dot represents the percentage of TSSA from a single newborn pup, with the horizontal lines representing the mean value for each genotype (n = 12). **C:** Representative sections immunostained for Ki67 of newborn (P0) lungs from $HB^{+/+}$;$Tgf\alpha^{+/+}$ (a), $HB^{+/+}$;$Tgf\alpha^{-/-}$ (b), $HB^{del/+}$;$Tgf\alpha^{-/-}$ (c), $HB^{del/del}$;$Tgf\alpha^{+/+}$ (d), and $HB^{del/del}$;$Tgf\alpha^{+/-}$ (e). **D:** Comparison of percentage of Ki67-positive cells in total lung cells of newborn lungs from $HB^{+/+}$;$Tgf\alpha^{+/+}$, $HB^{+/+}$;$Tgf\alpha^{-/-}$, $HB^{del/+}$;$Tgf\alpha^{-/-}$, $HB^{del/del}$;$Tgf\alpha^{+/+}$ and $HB^{del/del}$;$Tgf\alpha^{+/-}$. Each dot represents the percentage of Ki67-positive cells/total cells from a single newborn pup, with the horizontal lines representing the mean value for each genotype (n = 8). For abbreviations, see list. Original magnification, ×200. Scale bar = 100 μm in A,C.

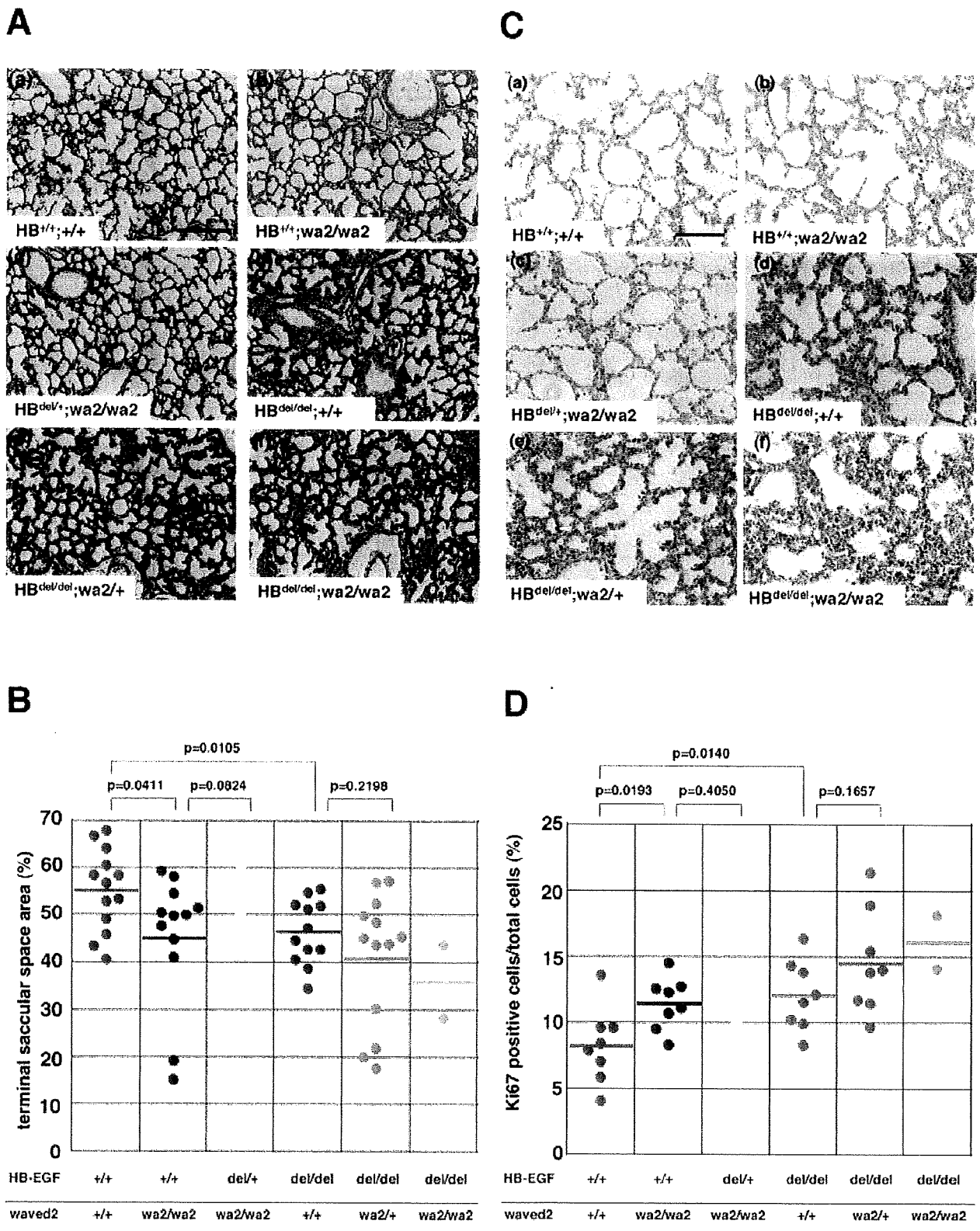
A
C
B
D
HB+/+;+/+
HB+/+;wa2/wa2
HBdel/+;wa2/wa2
HBdel/del;+/+
HBdel/del;wa2/+
HBdel/del;wa2/wa2
p=0.0105
p=0.0411
p=0.0824
p=0.2198
terminal saccular space area (%)
p=0.0140
p=0.0193
p=0.4050
p=0.1657
Ki67 positive cells/total cells (%)
HB-EGF +/+ +/+ del/+ del/del del/del del/del
waved2 +/+ wa2/wa2 wa2/wa2 +/+ wa2/+ wa2/wa2

Fig. 7.

processes of cardiac valve development and lung saccular development remain unclear. It will be interesting to investigate whether a common mechanism underlies in these two HB-EGF–mediated developmental processes.

A physiological role of TGFα in lung saccular development has remained unknown up to this study. A recent study showed that conditional transgenic mice in which TGFα was overexpressed in prenatal lung had exhibited abnormal lung morphology at birth, characterized by mesenchymal thickening, vascular remodeling, and poor apposition of capillaries to distal airspaces. Moreover, these mice died within a week after birth. In those lungs, proliferation was enhanced and the number of type II epithelial cells was increased (Kramer et al., 2007). By contrast, lung abnormalities have not been reported in TGFα null mice until now. In this study, we show that TGFα has an inhibitory function milder than HB-EGF, and TGFα functions synergistically with HB-EGF in perinatal distal lung development. There was a slight difference in quantitative comparison of TSSA, and there was an insignificant difference in the score of Ki67-positive cells between $TGF\alpha^{+/+}$ and $TGF\alpha^{-/-}$ lungs. Most of the $TGF\alpha^{-/-}$ lungs are morphologically normal, and only a few $TGF\alpha^{-/-}$ lungs exhibited abnormalities characterized by thickened saccular wall and poorly inflated sacculi. However, $HB^{del/del}$; $TGF\alpha^{+/-}$ lungs showed reduced TSSA more frequently and more cell proliferation than $HB^{del/del}$; $TGF\alpha^{+/+}$ lungs with statistical significance. To our knowledge, it is the first evidence that TGFα contributes to normal perinatal lung development. Together with the recent study of the conditional TGFα transgenic mice (Kramer et al., 2007), these results suggest that a delicate regulation of TGFα expression is important for normal lung formation in this stage. Namely, the absence of TGFα induces mild reduction of proliferation as shown in this study, while an excessive expression of TGFα in this stage also results in abnormal saccular morphology caused by hyperproliferation of the saccular cells (Kramer et al., 2007).

TGFα is expressed in bronchioles and saccular epithelia in late gestational lungs (Strandjord et al., 1993, 1994, 1995; Ruocco et al., 1996). It was reported that the expression is decreased by 50% during the transition from the canalicular (E19–E20) to the saccular (E21) stage in late-term fetal rat lung (Kubiak et al., 1992). This change of expression is consistent with our chronological analysis of TGFα mRNA expression by RT-PCR, which revealed that TGFα expression decreases in the prenatal saccular stage and rapidly increases after birth. On the other hand, HB-EGF expression is not down-regulated but rather up-regulated in the prenatal stage. This difference in expression patterns between HB-EGF and TGFα can explain the difference of phenotypic penetrance between $HB^{del/del}$ and $TGF\alpha^{-/-}$ lungs at birth. During prenatal stage, HB-EGF is expressed increasingly and mainly functions in the sacculi, while at birth, both HB-EGF and TGFα are expressed, such that in $TGF\alpha^{-/-}$ lungs, endogenous HB-EGF compensates for the lost function of TGFα during normal perinatal distal lung development.

In perinatal mouse lungs, the expression pattern of other EGFR ligands, including AR, EPR, and BTC, except for EGF, is essentially similar to TGFα. Their expressions are generally once decreased in the prenatal saccular stage. These results also suggest that HB-EGF is the primary factor among EGFR ligands responsible for normal prenatal distal lung development, and that after birth, HB-EGF may regulate cell proliferation synergistically with other EGF family ligands as well as with TGFα. It still remains unclear why the expression of other EGF family ligands except for HB-EGF initially decreases in the prenatal saccular stage during normal lung saccular development. Further study is necessary to clarify the developmental significance of those unique expression profiles and the molecular mechanisms regulating the EGFR ligands in lung saccular development during the saccular stage.

EGFR and ErbB4 are two known cognate receptors for HB-EGF (Higashiyama et al., 1991; Elenius et al., 1997). Loss of EGFR leads to an overall pulmonary malformation, including impaired branching, deficient alveolarization, reduced surfactant protein, and a marked reduction in alveolar volume in the lung (Miettinen et al., 1995; Sibilia and Wagner, 1995; Miettinen et al., 1997). These phenotypes are in part similar to that of HB-EGF null mice. Although ErbB4 null mice die at mid-gestation (E10.5) due to central nervous system and cardiac malformations (Gassmann et al., 1995), ErbB4 null mice genetically rescued from embryonic lethality by heart-specific expression of human ErbB4 are known to reach adulthood. Any lung defects has not been described in these mice (Tidcombe et al., 2003). These studies suggest that EGFR is a possible major receptor for HB-EGF at least in this process.

In this study, we genetically analyze the relationship between HB-EGF and EGFR using waved 2 mice, a hypomorphic EGFR mutant strain. Some $HB^{+/+}$; wa2/wa2 lungs exhibited a reduced TSSA and a significantly higher score in cell proliferation, compared with wild-type lungs. Moreover, $HB^{del/del}$; wa2/+ lungs exhibited a reduced TSSA more frequently and higher score of cell prolif-

**Fig. 7.** Comparison of TSSA and cell proliferation in double mutants of HB-EGF and waved 2 newborn pups. **A:** Representative hematoxylin/eosin-stained sections of newborn lungs from $HB^{+/+}$;+/+ (a), $HB^{+/+}$;wa2/wa2 (b), $HB^{del/+}$;wa2/wa2 (c), $HB^{del/del}$;+/+ (d), $HB^{del/del}$;wa2/+ (e), and $HB^{del/del}$;wa2/wa2 (f). **B:** Comparison of TSSA of newborn lung alveoli from $HB^{+/+}$;+/+, $HB^{+/+}$;wa2/wa2, $HB^{del/+}$;wa2/wa2, $HB^{del/del}$;+/+, $HB^{del/del}$;wa2/+, and $HB^{del/del}$;wa2/wa2. Each dot represents the percentage of TSSA from a single newborn pup, with the horizontal lines representing the mean value for each genotype (n = 12–13 in $HB^{+/+}$;+/+, $HB^{+/+}$;wa2/wa2, $HB^{del/+}$;wa2/wa2, $HB^{del/del}$;+/+ and $HB^{del/del}$;wa2/+, n = 2 in $HB^{del/del}$;wa2/wa2). **C:** Representative sections immunostained for Ki67 of newborn lung alveoli from $HB^{+/+}$;+/+ (a), $HB^{+/+}$;wa2/wa2 (b), $HB^{del/+}$;wa2/wa2 (c), $HB^{del/del}$;+/+ (d), $HB^{del/del}$;wa2/+ (e), and $HB^{del/del}$;wa2/wa2 (f). **D:** Comparison of percentage of Ki67-positive cells in total lung cells in newborn (P0) lungs from $HB^{+/+}$;+/+, $HB^{+/+}$;wa2/wa2, $HB^{del/+}$;wa2/wa2, $HB^{del/del}$;+/+, $HB^{del/del}$;wa2/+, and $HB^{del/del}$;wa2/wa2. Each dot represents the percentage of Ki67-positive cells/total cells from a single newborn pup, with the horizontal lines representing the mean value for each genotype (n = 8, in $HB^{+/+}$;+/+, $HB^{+/+}$;wa2/wa2, $HB^{del/+}$;wa2/wa2, $HB^{del/del}$;+/+ and $HB^{del/del}$;wa2/+, n = 2 in $HB^{del/del}$;wa2/wa2). For abbreviations, see list. Original magnification, ×200. Scale bar = 100 μm in A,C.

eration than $HB^{del/del}$; +/+ lungs, although without statistical significance. These results suggest that EGFR is involved in HB-EGF–mediated perinatal distal lung development. However, these results do not deny the possibilities that, as well as EGFR, other ErbB family receptors (for example, ErbB4) are also required for normal lung development. The differences in TSSA and proliferation rate between each genotype group of HB-EGF and waved 2 double-mutant mice were much less than the case of HB-EGF and TGFα double-mutant analysis. Furthermore, even waved 2 mice exhibited nearly normal lung morphology at birth and survived. Thus, it will be necessary to study the comprehensive relationship between HB-EGF and ErbB family receptors in lung development.

Almost all HB-EGF null newborns with C57BL/6J backgrounds used in this study died shortly after birth. Impaired development in $HB^{del/del}$ lungs is one possible cause of this early death of the HB-EGF null newborns. However, the penetrance of this lung phenotype is relatively low, and it was observed in only approximately half of $HB^{del/del}$ lungs, whereas the remaining $HB^{del/del}$ lungs were similar to the wild-type morphology. Although it was reported that $HB^{del/del}$ lungs showed immature lung differentiation (Jackson et al., 2003), our immunohistochemical analysis showed no remarkable change in pro-surfactant protein C expression between $HB^{+/+}$ and $HB^{del/del}$ lungs, ruling out the possibility of immature differentiation as a cause of respiratory distress. We unfortunately failed to follow the morphological change in $HB^{del/del}$ lungs after birth because of the severe perinatal lethality of HB-EGF null mice. Thus, it is possible that those lungs of $HB^{del/del}$ with apparently normal morphology rapidly deteriorate after birth, or that we do not notice other hidden severe defects than lungs in HB-EGF null mice. Despite our efforts, it still remains unclear what really causes the early death of HB-EGF null mice.

In conclusion, in the present study, we demonstrated that HB-EGF signaling contributes to perinatal distal lung development. HB-EGF functions synergistically with TGFα, and EGFR signaling regulates the decelerated cell proliferation in the perinatal distal lung. Nonetheless, the complete network of molecular mechanisms regulating these processes remains to be elucidated.

## EXPERIMENTAL PROCEDURES

### Mice

The generation of HB-EGF null mice ($HB^{del/del}$) has been previously described (Iwamoto et al., 2003). These mice were back-crossed for eight or nine generations onto a background of C57BL/6J strain. TGFα null and waved 2 mice were purchased from Jackson Laboratory. TGFα null mice were maintained on a background of the C57BL/6J strain. Waved 2 mice with a mixed background of C57BL/6JEi and C3H/HeSnJ when purchased, were back-crossed for four or five generations onto a background of C57BL/6J strain. For producing double-mutant mice of TGFα and HB-EGF, or waved 2 and HB-EGF, HB-EGF heterozygous or null mice that were back-crossed for three or four generations onto a background of C57/BL/6J were mated with mice described above. The finding of a vaginal plug was considered as E0.5. Timed pregnant females were killed, and embryos dissected from the uteri were placed in phosphate-buffered saline (PBS). Mice were classified as P0 when birth was witnessed and their breathing activities visualized. All mice used in this investigation were housed in Osaka University Research Institute for Microbial Diseases Animal Care Facility according to the Institutional guidelines for laboratory animals. The use and treatment of animals was approved by the Institutional Biosafety Committee on Biological Experimentation at Osaka University and the Institutional Animal Experimentation Committee at Osaka University.

### Reverse Transcription PCR

Total RNA from tissues was isolated using ISOGEN (Invitrogen). One microgram of total RNA was reverse transcribed using a reverse transcriptase, ReverTra Ace (TOYOBO). PCR analysis was performed by using KOD dash (TOYOBO) for HB-EGF (98°C for 10 sec, 60°C for 2 sec, 74°C for 30 sec; 30 cycles), EGF (98°C for 10 sec, 65°C for 2 sec, 74°C for 30 sec; 30 cycles) and glyceraldehydes-3-phosphate dehydrogenase (GAPDH; 98°C for 10 sec, 57°C for 2 sec, 74°C for 30 sec; 30 cycles), and by using KOD plus (TOYOBO) for TGFα (94°C for 15 sec, 68°C for 1 min; 32 cycles), AR (94°C for 15 sec, 68°C for 1 min; 35 cycles), EPR (94°C for 15 sec, 58°C for 30 sec, 68°C for 30 sec; 35 cycles) and BTC (94°C for 15 sec, 60°C for 30 sec, 68°C for 1 min; 33 cycles). The gene-specific primers are as follows: HB-EGF (5′-ATGAAGCTGCTGCCGTCGGT-3′ and 5′-TCAGTGGGAGCTAGCCACGC-3′), TGFα (5′-ATGGTCCCCGCGACCGGACAGCTCGCTCTG-3′ and 5′-ATCTTCAGACCACTGTCTCAGAGTGGCAGC-3′), AR (5′-ATGAGAACTCCGCTGCTACCGCTGGCGCGC-3′ and 5′-CAGCTAGGCAATGGCGTGCACAGTCCCATT-3′), EPR (5′-CAGGCAGTTATCAGCACAAC-3′, and 5′-CCTTGTCCGTAACTTGATGG-3′), BTC (5′-ATGGACCCAACAGCCCCGGGTAGCAGTGTC-3′ and 5′-TAACCGTTAAGCAATATTGGTCTCTTGAAT-3′), EGF (5′-ATGCCCTGGGGCCGAAGGCCAACCTGGCTG-3′ and 5′-TGTAAGCGTGGCTTCCTTCGCCACTGTCCT-3′), and GAPDH (5′-ACCACAGTCCATGCCATCAC-3′, and 5′-TCCACCACCCTGTTGCTGTA-3′). The optimal cycle number for each gene was determined empirically under unsaturating conditions.

### *LacZ* Staining

Dissected newborn lungs were fixed by perfusion of 0.5% glutaraldehyde-2 mM $MgCl_2$ in PBS (pH 7.4) for 1 hr at 4°C before equilibrating in a sucrose solution (30% sucrose-2 mM $MgCl_2$ in PBS, pH 7.4) overnight at 4°C. Sucrose-infused tissues were embedded in OCT compound and then frozen at −80°C. Eight μm sections were fixed again with 4% paraformaldehyde-2 mM $MgCl_2$ in PBS (pH 7.4) for 10 min at 4°C and then stained with X-gal reaction buffer (containing 35 mM potassium ferrocyanide, 35 mM potassium ferricyanide, 2 mM $MgCl_2$, 0.02% Nonidet P-40, 0.01% Na deoxycholate and 1 mg/ml 5-bromo-4-chloro-3-indolyl-β-D-galactoside in PBS, pH7.4) overnight at 37°C. For *LacZ*

staining of adult lungs, procedures of 0.5% glutaraldehyde perfusion and equilibrating in a sucrose solution were omitted. *LacZ*-stained tissues were counterstained with nuclear fast red.

### Hematoxylin and Eosin Staining

Newborns were killed by lethal injection of pentobarbital. Thoraces of embryos and newborns were isolated by decapitation and transection at the level of the liver. Skin and soft tissues were removed and then the intact thoraces were immersed in 4% paraformaldehyde in PBS (pH 7.4) at 4°C for 30 hours. After fixation, heart and lung en bloc was carefully isolated from thoracic cavity without punching the lung or diaphragm to minimize any collapse of the lung. The fixed lungs were dehydrated in graded concentration series of ethanol, and embedded in paraffin. Coronal sections were cut at 4 μm thickness and stained with hematoxylin and eosin.

### Lung Morphometry

TSSA were measured as previously described (Shi et al., 1999; Zhao et al., 2001; Yu et al., 2004) by using Adobe Photoshop software. Multiple measurements were performed on randomly selected 0.08-$mm^2$ image fields acquired from two separate sections greater than 50 μm apart from more than 12 fetal or newborn distal lungs of each genotype (Atkinson et al., 2005). Five fields were selected from one section, including two fields from the cranial lobe of the right lung, two fields from the left lung, and one field from the caudal lobe of the right lung. Fields containing large airways and vessels were avoided. The proportion of lung comprising terminal saccular spaces was calculated as percentage of the total examined area of the lung section.

### Measurement of Wet-to-Dry Lung Weight Ratio

After body weights were recorded, newborn lungs were removed intact from the thoracic cavity, blotted free of excess fluid, and weighed. Wet lungs were baked for 24 hr at 65°C. Dried lungs were then weighed (Kramer et al., 2007).

### Immunohistochemistry and Quantification

Four-μm lung sections were deparaffinized in xylene, followed by rehydration in series of concentrations of ethanol. The endogenous hydrogen peroxidase was quenched with 6% $H_2O_2$ for 5 min. Sections were incubated with Ki67 rabbit polyclonal antibody (NCL-Ki67p, Novocastra) diluted 1:500 in blocking solution Block Ace (Dainihon Seiyaku) overnight at 4°C, and then incubated with biotinylated goat anti-rabbit secondary antibody (Vector Laboratories) diluted 1:200 for 30 min at room temperature. Staining was developed using a R.T.U. Vectastain kit (Vector Laboratories) and a diaminobenzidine (DAB) substrate (Merck). Sections were counterstained lightly with hematoxylin. Apoptosis was examined by TUNEL according to the manufacturer's protocol (Promega). After immunostaining with Ki67 or TUNEL staining, randomly selected 0.019 or 0.037 $mm^2$ image fields acquired from two separate sections greater than 50 μm apart from fetal or newborn distal lungs of each genotype (in total, more than 10 fields from 2 sections of each sample), was captured with the Axiocam digital camera and Axiovision software (Zeiss). An average of 3,285 cells per animal (ranging from 1,543 to 6,022 cells per animal) were counted for this analysis. DAB-stained cells were counted as Ki67- or TUNEL-positive on photographs. The proportion of DAB-positive–stained cells per total cell number was represented as the amount of proliferation or apoptosis.

For pro-surfactant C immunohistochemistry, 4-μm lung sections were deparaffinized in xylene, followed by rehydration in series of concentrations of ethanol. The endogenous hydrogen peroxidase was quenched with 3% $H_2O_2$ in methanol for 15 min. Sections were incubated with rabbit anti-prosurfactant protein-C (proSP-C) antibody (Chemicon) diluted 1:2,000 in blocking solution (4% goat serum and 0.2% TriotnX-100 in PBS) overnight at 4°C, and then incubated with biotinylated goat anti-rabbit secondary antibody (Vector laboratories) diluted 1:200 for 30 min at room temperature. Staining was developed using the aforementioned R.T.U. Vectastain kit and DAB substrate. Sections were counterstained lightly with Hematoxylin.

### Data Analysis

Data are presented as means ± SE. Statistical significance was assessed with Student's *t*-test for paired data, or when necessary, the unpaired *t*-test for unequal variances. A value of $P < 0.05$ was considered statistically significant.

## ACKNOWLEDGMENTS

We thank M. Hamaoka and T. Kawaguchi for their technical assistance and advice. R.I. and E.M. were funded by grants-in-aid from the Ministry of Education, Culture, Sports, Science, and Technology and E.M. received a grant-in-aid from Takeda Science Foundation.

## REFERENCES

Atkinson JJ, Holmbeck K, Yamada S, Birkedal-Hansen H, Parks WC, Senior RM. 2005. Membrane-type 1 matrix metalloproteinase is required for normal alveolar development. Dev Dyn 232:1079–1090.

Burri PH. 1999. Lung development and pulmonary angionenesis. In: Gaultier C, Bourbon J, Post M, editors. Lung disease. New York: Oxford University Press. p 122–151.

Elenius K, Paul S, Allison G, Sun J, Klagsbrun M. 1997. Activation of HER4 by heparin-binding EGF-like growth factor stimulates chemotaxis but not proliferation. EMBO J 16:1268–1278.

Fowler KJ, Walker F, Alexander W, Hibbs ML, Nice EC, Bohmer RM, Mann GB, Thumwood C, Maglitto R, Danks JA, et al. 1995. A mutation in the epidermal growth factor receptor in waved-2 mice has a profound effect on receptor biochemistry that results in impaired lactation. Proc Natl Acad Sci U S A 92:1465–1469.

Gassmann M, Casagranda F, Orioli D, Simon H, Lai C, Klein R, Lemke G. 1995. Aberrant neural and cardiac development in mice lacking the ErbB4 neuregulin receptor. Nature 378:390–394.

Goishi K, Higashiyama S, Klagsbrun M, Nakano N, Umata T, Ishikawa M, Mekada E, Taniguchi N. 1995. Phorbol ester induces the rapid processing of cell surface heparin-binding EGF-like growth factor: conversion from juxta-

crine to paracrine growth factor activity. Mol Biol Cell 6:967–980.
Harris RC, Chung E, Coffey RJ. 2003. EGF receptor ligands. Exp Cell Res 284:2–13.
Hashimoto K, Higashiyama S, Asada H, Hashimura E, Kobayashi T, Sudo K, Nakagawa T, Damm D, Yoshikawa K, Taniguchi N. 1994. Heparin-binding epidermal growth factor-like growth factor is an autocrine growth factor for human keratinocytes. J Biol Chem 269:20060–20066.
Higashiyama S, Abraham JA, Miller J, Fiddes JC, Klagsbrun M. 1991. A heparin-binding growth factor secreted by macrophage-like cells that is related to EGF. Science 251:936–939.
Holbro T, Hynes NE. 2004. ErbB receptors: directing key signaling networks throughout life. Annu Rev Pharmacol Toxicol 44:195–217.
Iwamoto R, Mekada E. 2000. Heparin-binding EGF-like growth factor: a juxtacrine growth factor. Cytokine Growth Factor Rev 11:335–344.
Iwamoto R, Mekada E. 2006. ErbB and HB-EGF signaling in heart development and function. Cell Struct Funct 31:1–14.
Iwamoto R, Yamazaki S, Asakura M, Takashima S, Hasuwa H, Miyado K, Adachi S, Kitakaze M, Hashimoto K, Raab G, Nanba D, Higashiyama S, Hori M, Klagsbrun M, Mekada E. 2003. Heparin-binding EGF-like growth factor and ErbB signaling is essential for heart function. Proc Natl Acad Sci U S A 100:3221–3226.
Jackson LF, Qiu TH, Sunnarborg SW, Chang A, Zhang C, Patterson C, Lee DC. 2003. Defective valvulogenesis in HB-EGF and TACE-null mice is associated with aberrant BMP signaling. EMBO J 22:2704–2716.
Kimura R, Iwamoto R, Mekada E. 2005. Soluble form of heparin-binding EGF-like growth factor contributes to retinoic acid-induced epidermal hyperplasia. Cell Struct Funct 30:35–42.
Kramer EL, Deutsch GH, Sartor MA, Hardie WD, Ikegami M, Korfhagen TR, Le Cras TD. 2007. Perinatal increases in TGF-{alpha} disrupt the saccular phase of lung morphogenesis and cause remodeling: microarray analysis. Am J Physiol Lung Cell Mol Physiol 293:L314–L27.
Kubiak J, Mitra MM, Steve AR, Hunt JD, Davies P, Pitt BR. 1992. Transforming growth factor-alpha gene expression in late-gestation fetal rat lung. Pediatr Res 31:286–290.
Luetteke NC, Phillips HK, Qiu TH, Copeland NG, Earp HS, Jenkins NA, Lee DC. 1994. The mouse waved-2 phenotype results from a point mutation in the EGF receptor tyrosine kinase. Genes Dev 8:399–413.
Massague J, Pandiella A. 1993. Membrane-anchored growth factors. Annu Rev Biochem 62:515–541.
Miettinen PJ, Berger JE, Meneses J, Phung Y, Pedersen RA, Werb Z, Derynck R. 1995. Epithelial immaturity and multiorgan failure in mice lacking epidermal growth factor receptor. Nature 376:337–341.
Miettinen PJ, Warburton D, Bu D, Zhao JS, Berger JE, Minoo P, Koivisto T, Allen L, Dobbs L, Werb Z, Derynck R. 1997. Impaired lung branching morphogenesis in the absence of functional EGF receptor. Dev Biol 186:224–236.
Mine N, Iwamoto R, Mekada E. 2005. HB-EGF promotes epithelial cell migration in eyelid development. Development 132:4317–4326.
Miyamoto S, Yagi H, Yotsumoto F, Kawarabayashi T, Mekada E. 2006. Heparin-binding epidermal growth factor-like growth factor as a novel targeting molecule for cancer therapy. Cancer Sci 97:341–347.
Piepkorn M, Pittelkow MR, Cook PW. 1998. Autocrine regulation of keratinocytes: the emerging role of heparin-binding, epidermal growth factor-related growth factors. J Invest Dermatol 111:715–721.
Raab G, Klagsbrun M. 1997. Heparin-binding EGF-like growth factor. Biochim Biophys Acta 1333:F179–F199.
Roth-Kleiner M, Hirsch E, Schittny JC. 2004. Fetal lungs of tenascin-C-deficient mice grow well, but branch poorly in organ culture. Am J Respir Cell Mol Biol 30:360–366.
Ruocco S, Lallemand A, Tournier JM, Gaillard D. 1996. Expression and localization of epidermal growth factor, transforming growth factor-alpha, and localization of their common receptor in fetal human lung development. Pediatr Res 39:448–455.
Shi W, Heisterkamp N, Groffen J, Zhao J, Warburton D, Kaartinen V. 1999. TGF-beta3-null mutation does not abrogate fetal lung maturation in vivo by glucocorticoids. Am J Physiol 277:L1205–L1213.
Shirakata Y, Kimura R, Nanba D, Iwamoto R, Tokumaru S, Morimoto C, Yokota K, Nakamura M, Sayama K, Mekada E, Higashiyama S, Hashimoto K. 2005. Heparin-binding EGF-like growth factor accelerates keratinocyte migration and skin wound healing. J Cell Sci 118:2363–2370.
Sibilia M, Wagner EF. 1995. Strain-dependent epithelial defects in mice lacking the EGF receptor. Science 269:234–238.
Strandjord TP, Clark JG, Hodson WA, Schmidt RA, Madtes DK. 1993. Expression of transforming growth factor-alpha in mid-gestation human fetal lung. Am J Respir Cell Mol Biol 8:266–272.
Strandjord TP, Clark JG, Madtes DK. 1994. Expression of TGF-alpha, EGF, and EGF receptor in fetal rat lung. Am J Physiol 267:L384–L389.
Strandjord TP, Clark JG, Guralnick DE, Madtes DK. 1995. Immunolocalization of transforming growth factor-alpha, epidermal growth factor (EGF), and EGF-receptor in normal and injured developing human lung. Pediatr Res 38:851–856.
Ten Have-Opbroek AA. 1991. Lung development in the mouse embryo. Exp Lung Res 17:111–130.
Tidcombe H, Jackson-Fisher A, Mathers K, Stern DF, Gassmann M, Golding JP. 2003. Neural and mammary gland defects in ErbB4 knockout mice genetically rescued from embryonic lethality. Proc Natl Acad Sci U S A 100:8281–8286.
Yamazaki S, Iwamoto R, Saeki K, Asakura M, Takashima S, Yamazaki A, Kimura R, Mizushima H, Moribe H, Higashiyama S, Endoh M, Kaneda Y, Takagi S, Itami S, Takeda N, Yamada G, Mekada E. 2003. Mice with defects in HB-EGF ectodomain shedding show severe developmental abnormalities. J Cell Biol 163:469–475.
Yu H, Wessels A, Chen J, Phelps AL, Oatis J, Tint GS, Patel SB. 2004. Late gestational lung hypoplasia in a mouse model of the Smith-Lemli-Opitz syndrome. BMC Dev Biol 4:1.
Zhao J, Chen H, Peschon JJ, Shi W, Zhang Y, Frank SJ, Warburton D. 2001. Pulmonary hypoplasia in mice lacking tumor necrosis factor-alpha converting enzyme indicates an indispensable role for cell surface protein shedding during embryonic lung branching morphogenesis. Dev Biol 232:204–218.

Biochemical and Biophysical Research Communications 393 (2010) 55–60

Contents lists available at ScienceDirect

Biochemical and Biophysical Research Communications

journal homepage: www.elsevier.com/locate/ybbrc

# Identification of genes related to heart failure using global gene expression profiling of human failing myocardium

Kyung-Duk Min [a], Masanori Asakura [a,*], Yulin Liao [c], Kenji Nakamaru [d], Hidetoshi Okazaki [a], Tomoko Takahashi [d], Kazunori Fujimoto [d], Shin Ito [a], Ayako Takahashi [a], Hiroshi Asanuma [e], Satoru Yamazaki [b], Tetsuo Minamino [g], Shoji Sanada [a], Osamu Seguchi [a], Atsushi Nakano [a], Yosuke Ando [d], Toshiaki Otsuka [d], Hidehiko Furukawa [d], Tadashi Isomura [f], Seiji Takashima [g], Naoki Mochizuki [b], Masafumi Kitakaze [a]

[a] *Department of Cardiovascular Medicine, Osaka, Japan*
[b] *Research Institute, National Cardiovascular Center, Osaka, Japan*
[c] *Department of Pathophysiology, Southern Medical University, Guangzhou 510515, China*
[d] *R&D Division, Daiichi Sankyo Co., Ltd., Tokyo, Japan*
[e] *Department of Emergency Room Medicine, Kinki University School of Medicine, Sayama, Osaka, Japan*
[f] *Hayama Heart Center, Hayama, Kanagawa, Japan*
[g] *Department of Cardiovascular Medicine, Osaka University Graduate School of Medicine, Suita, Osaka, Japan*

ARTICLE INFO

*Article history:*
Received 12 January 2010
Available online 25 January 2010

*Keywords:*
Gene expression
cDNA microarray
Heart failure
Clinical parameter

ABSTRACT

Although various management methods have been developed for heart failure, it is necessary to investigate the diagnostic or therapeutic targets of heart failure. Accordingly, we have developed different approaches for managing heart failure by using conventional microarray analyses. We analyzed gene expression profiles of myocardial samples from 12 patients with heart failure and constructed datasets of heart failure-associated genes using clinical parameters such as pulmonary artery pressure (PAP) and ejection fraction (EF). From these 12 genes, we selected four genes with high expression levels in the heart, and examined their novelty by performing a literature-based search. In addition, we included four G-protein-coupled receptor (GPCR)-encoding genes, three enzyme-encoding genes, and one ion-channel protein-encoding gene to identify a drug target for heart failure using *in silico* microarray database. After the *in vitro* functional screening using adenovirus transfections of 12 genes into rat cardiomyocytes, we generated gene-targeting mice of five candidate genes, namely, *MYLK3*, *GPR37L1*, *GPR35*, *MMP23*, and *NBC1*. The results revealed that systolic blood pressure differed significantly between *GPR35*-KO and *GPR35*-WT mice as well as between *GPR37L1*-Tg and *GPR37L1*-KO mice. Further, the heart weight/body weight ratio between *MYLK3*-Tg and *MYLK3*-WT mice and between *GPR37L1*-Tg and *GPR37L1*-KO mice differed significantly. Hence, microarray analysis combined with clinical parameters can be an effective method to identify novel therapeutic targets for the prevention or management of heart failure.



## Introduction

Heart failure is a multi-factorial condition with increasing prevalence worldwide; further, a significant increase has been observed in the mortality rate and economic impact associated with this condition. In the last 20 years, substantial development of treatment for heart failure, including angiotensin-converting-enzyme inhibitors [1] and beta-blockers [2,3], has greatly improved the prognosis of the patients with heart failure. However, despite these rapid advancements in the management of heart failure, effective treatment of end-stage heart failure without providing ventricular assistance or heart transplantation is still difficult. Investigation of new and unexplored targets for the prevention or treatment of heart failure is warranted. Global gene expression analysis using microarray technique has been used in the last decade to identify biomarkers or drug targets for heart failure [4–10]. Several gene expression signatures of heart failure have been identified by analyzing independent microarray datasets [11,12]. However, most of these analyses did not consider the severity of heart failure. Because the severity of heart failure may quantitatively reflect the expression levels of genes such as the natriuretic

* Corresponding author. Address: Department of Research and Development of Clinical Research, National Cardiovascular Center, 5-7-1 Fujishirodai, Suita, Osaka 565-8565, Japan.
*E-mail address:* masakura@hsp.ncvc.go.jp (M. Asakura).

0006-291X/$ - see front matter © 2010 Elsevier Inc. All rights reserved.
doi:10.1016/j.bbrc.2010.01.076

peptide-encoding gene, expression analysis combined with the severity of heart failure could be an appropriate method to identify heart failure-related genes. However, microarray analysis of genes expressed in failing myocardium while considering the severity of heart failure has not yet been reported.

Hence, we investigated the genes whose expression level correlated with clinical parameters such as pulmonary artery pressure (PAP), left ventricular ejection fraction (EF), and brain natriuretic peptide (BNP) mRNA level. Using this approach, we identified cardiac myosin light chain kinase as a novel heart failure-related gene [13]. Here, we describe newly identified several genes whose expression correlated with clinical parameters and additional genes encoding G-protein-coupled receptor genes (GPCRs), other enzymes and ion-channel proteins, and performed the functional analysis of these heart failure-related genes. This novel strategy involving the use of clinical parameters might find potential applications for the identification of disease-associated genes that could not be detected using conventional microarray techniques.

## Materials and methods

*Patient characteristics.* We recruited 12 patients (11 males and 1 female) with heart failure and obtained written informed consent from them. The patients were diagnosed with severe chronic heart failure due to various cardiac diseases such as dilated cardiomyopathy and myocardial infarction [13]. The average age of patients was 55 ± 13 years. The plasma level of BNP, which is the best marker for the severity of heart failure, ranged from 80 to 2710 pg/ml. The mean PAP measured using a Swan-Ganz catheter 1–4 weeks before the operation varied between 16 and 59 mmHg. The average of EF determined by echocardiography on the day before the operation was 32.5% ± 12.4%.

*Microarray analysis and subsequent in silico functional analysis.* RNA was extracted from myocardium samples of 12 heart failure patients who had undergone either Batista or Dor surgeries. RNA samples of non-failing hearts were purchased from Biochain, Inc. Complementary RNA (cRNA) was prepared from RNA samples and hybridized to HG-U95 Affymetrix GeneChip (Affymetrix, US). The expression data were analyzed using Microarray Analysis Suite version 5.0 software. Among all the genes detected on the microarray, we selected the genes whose expression was significantly different in the failing and non-failing myocardial samples ($p < 0.005$). From these genes, we selected genes whose expression was correlated with PAP, EF, and BNP mRNA level, with 0.7 being the cutoff value of the correlation coefficient. The values of PAP, EF, and BNP mRNA level used for the correlation analysis were normalized to their median during the measurements. Subsequently, the functional analysis of datasets was performed using Ingenuity Pathway Analysis (Ingenuity® Systems; www.ingenuity.com), and the biological functions most significant to the dataset were identified.

*Cell culture.* Cardiomyocytes were harvested before the experiments from 2- to 3-day-old neonatal rats and cultured as described in previous studies [14]. Briefly, primary cardiomyocytes isolated from neonatal rats were grown in Dulbecco's modified Eagle medium/F12 (Gibco) supplemented with 10% fetal calf serum for 72 h, and then cultured in a serum-free condition for 24 h.

*Adenovirus generation and transfection.* Adenovirus constructs encoding the genes of interest were generated using the ViraPower Adenoviral Expression System (Invitrogen, US) according to the manufacturer's method. Adenovirus vectors were transfected to cultured cardiomyocytes for 12 h according to the published protocol.

*In vitro functional analysis of genes.* Cultured rat cardiomyocytes were infected by adenovirus vectors. After 24 h, hypertrophic reaction, cell viability, and cellular morphology were assessed. Hypertrophic reaction was determined by estimating the incorporation of [$^3$H]phenylalanine. In brief, [$^3$H]phenylalanine was added to the culture medium at the final concentration of 0.1 μCi/ml, and the cells were incubated for an additional 24 h. Then, the incorporation of [$^3$H]phenylalanine was determined by counting the radioactivity of each sample with a liquid scintillation counter. The viability of cardiomyocytes was evaluated by the Alamar blue assay according to the manufacturer's method. The morphology of cardiomyocytes was evaluated 24 h after adenovirus transfections.

*Generation of transgenic and knockout mice.* To generate transgenic mice, open reading frame of each gene, namely, *Mylk3*, *Gpr37l1*, or *Nbc1* was amplified from mouse cDNA by PCR, with Sal I site linker on each end, and cloned into Sal I site of alpha-MHC clone 26 vector. Then the DNAs used in the microinjections were released from the vector by digestion with NotI and were microinjected into fertilized eggs of mouse. Founder mice were identified by PCR analysis with appropriate primers. To develop *Gpr37l1* knockout mice, the targeting vector was assembled to replace the exon 1 and 2 by neomycin selection cassete resulting in the absence of *Gpr37l1* protein. W9.5 ES cells were electroporated with linearized targeting vector. ES cell clones with successful homologous recombination was determined by the PCR and subsequent direct sequence. From these targeted ES cells, the chimera mice were bred to C57 BL/6 females to generated F1 and F2 offsprings were obtained. The *Gpr37l1* null mice were determined by PCR genotyping of F2 offsprings. The knockout mice of *Gpr35* and *Mmp23* (*the* mouse ortholog of MMP23B) were purchased from Deltagen, Inc. (California, US).

*Invasive blood pressure measurement.* The phenotype of the gene-targeted mice was examined. Before sacrificing the mice, their hemodynamic parameters were evaluated. The mice were anesthetized and ventilated, and a Millar catheter was inserted via right carotid artery. The left-ventricular systolic and end-diastolic pressures were measured. Then, the mice were sacrificed and the weight of the whole body and heart was determined.

*Statistical analysis.* Unpaired Student's *t*-test was used for comparing the two groups. Results are expressed as means ± SEM, and *p* value less than 0.05 was considered statistically significant.

## Results

### *Identification of heart failure-related genes by expression analysis using clinical parameters*

We performed microarray analysis of the genes expressed in failing myocardium obtained from 12 patients with heart failure and the genes expressed in non-failing myocardium from two normal objects whose characteristics were reported in the previous study [13]. Although all patients were diagnosed with chronic heart failure, the plasma BNP level, which is an index of the severity of heart failure, ranged from 80 to 2710 pg/ml, suggesting that the severity of heart failure varied extensively among the patients. This marked difference in the severity of heart failure reflects the fact that the gene expression patterns in the 12 patients were not uniform, as shown in Fig. 1A. Thus, we analyzed gene expression profiles of failing myocardium using clinical parameters representing the severity of heart failure. We identified 166 and 194 genes whose expressions were correlated with PAP and BNP mRNA level, respectively (Fig. 1B and Supplementary Tables S1, S2). Among these, 49 genes correlated with both PAP and BNP mRNA level (Fig. 1C). The expression of only two genes, namely, *FMO2* and *LMAN1L*, correlated with the EF. We investigated the functional categories of these genes by performing Ingenuity Pathway Analysis. The number of genes in each group, functional categories, and

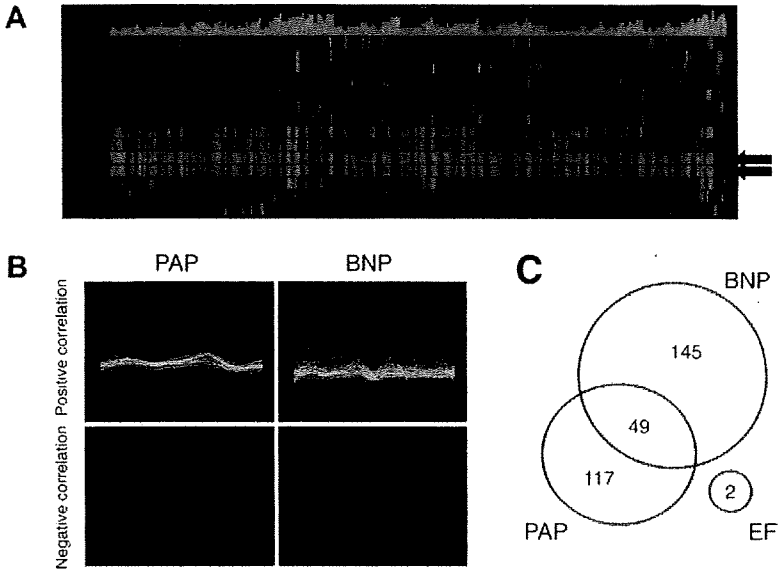


**Fig. 1.** The gene expression profile of human failing or non-failing myocardium. Gene expression levels of myocardial samples from 12 patients with severe heart failure and from two normals were analyzed using microarray. (A) Heat maps showing the genes with differential expression between the 12 failing myocardial samples and the two non-failing myocardial samples. Red color indicates upregulated gene expression. Green color indicates downregulated gene expression. Arrows indicate non-failing samples. (B) Expression profile of positively or negatively correlated genes to pulmonary artery pressure (PAP) or brain natriuretic peptide (BNP) mRNA level ($r > 0.7$). (C) Venn diagram of genes correlated with PAP, BNP, and ejection fraction.

**Table 1**
Datasets of genes whose expressions were correlated to clinical parameters.

| | PAP | EF | BNP mRNA level |
|---|---|---|---|
| *Positive correlation* | | | |
| Number | 124 | 1 | 175 |
| Function | Cardiovascular system development and function<br>Cell death | – | Cardiovascular system development and function<br>Cell cycle |
| Representative genes | *ARNT, MYOCD, SMARCA4*<br>*BGN, CFLAR, EEF2, MTPN* | *LMAN1L* | *BTG1, NPPA, NPPB, SERPNF1*<br>*CKS1B, DDR2, FCGR2B, FN1* |
| *Negative correlation* | | | |
| Number | 42 | 1 | 19 |
| Function | Skeletal and muscular system development and function<br>Cellular assembly and organization | – | Skeletal and muscular system development and function<br>Cellular assembly and organization |
| Representative genes | *PIK3R1, PRKAR1A, SLMAP*<br>*C19ORF20, RAB9A, SYNGAP1, TTN* | *FMO2* | *ACTC1, RBBP4, TTN* |

The function of gene sets was analyzed by Ingenuity Pathway Analysis.
PAP, pulmonary artery pressure; EF, ejection fraction; BNP, brain natriuretic peptide.

representative genes are shown in Table 1. Interestingly, both gene sets correlated positively with PAP and BNP mRNA level were most associated with the same functional category of "cardiovascular system development and function", although the included genes were different. Similarly, the gene sets correlated negatively with both PAP and BNP mRNA level had most association with common functional categories of "skeletal and muscular system development and function" and "cellular assembly and organization".

*Selection of 12 genes for in vitro screening*

Among the genes selected using clinical parameters, we selected those genes that showed high expression levels in the heart by performing microarray analysis. On the basis of their novelty determined by a literature-based search, we selected four genes for further investigation (Table 2). Concurrently, to identify possible drug targets, we included four orphan GPCRs and four additional genes (three enzyme-encoding genes and one ion-channel protein-encoding gene) in the further analysis. The *RHOQ* and *STK38* genes were selected based on their correlation with BNP mRNA level and PAP, respectively. *GPR161* and *NBC1* were selected owing to their high expression level in the heart. *GPR37L1*, *GPR35*, *F2RL2*, and *MMP23B* were selected because of their high expression level in the heart, and their association with the cardiac diseases-related genes listed in the database was determined by *in silico* analysis.

*Functional analysis of genes on the basis of adenovirus-mediated overexpression of proteins in neonatal rat cardiomyocytes*

To determine which of the selected genes were associated with the physiological functions of the heart, we first generated adenovirus vectors for each gene listed in Table 2 and transfected these vectors into neonatal rat cardiomyocytes. Next, we evaluated the hypertrophic reaction, viability, and morphology of the transfected cardiomyocytes. Among the 12 selected genes, three adenovirus-mediated genes decreased the incorporation of [$^3$H]phenylalanine in neonatal rat cardiomyocytes (Table 2); the expression of one

**Table 2**
*In vitro* functional screening of the 12 candidate genes.

| Probe set ID | Gene symbol | Gene name | Criteria for selection | *p* value | [$^3$H]PA intake | Fluorescence of Alamar blue | Cellular morphology |
|---|---|---|---|---|---|---|---|
| *Genes relevant to clinical parameters* | | | | | | | |
| 75678_at | *MYLK3* | Myosin light chain kinase 3 | Correlation with PAP ($r$ = 0.792) | 0.00262 | No change | No change | Spiking |
| 49333_at | *XPR1* | Xenotropic and polytropic retrovirus receptor | Correlation with PAP ($r$ = 0.765), GPCR, change in CHF | 0.00045 | No change | No change | No change |
| 38435_at | *PRDX4* | Peroxiredoxin 4 | Correlation with BNP ($r$ = 0.863) | 0.00024 | Increased | Decreased | No change |
| 45314_at | *SMOC2* | SPARC related modular calcium binding 2 | Correlation with both PAP and BNP ($r$ = 0.715 and 0.758, respectively) | 0.00444 | No change | No change | No change |
| *Genes encoding orphan GPCRs* | | | | | | | |
| 35544_at | *GPR37L1* | G-protein-coupled receptor 37 like 1 | Orphan GPCR, downregulated in CVD | >0.005 | Decreased | Decreased | Apoptosis |
| 31700_at | *GPR35* | G-protein-coupled receptor 35 | Orphan GPCR, upregulated in MI | 0.00216 | Decreased | Decreased | Hypertrophy |
| 45204_at | *F2RL2* | Coagulation factor II (thrombin) receptor-like 2 | GPCR, change in CVD | >0.005 | Increased | No change | No change |
| 40299_at | *GPR161* | G-protein-coupled receptor 161 | GPCR, expression in heart | >0.005 | Decreased | Decreased | No change |
| *Genes encoding interesting enzymes or ion-channels* | | | | | | | |
| 38950_at | *MMP23B* | Matrix metallopeptidase 23B | Family of MMP, change in CHF | >0.005 | No change | Decreased | No change |
| 35285_at | *NBC1* | $Na^+$–$HCO^{3-}$ cotransporter 1 | Expression in heart | >0.005 | No change | Decreased | No change |
| 87788_at | *RHOQ* | Ras homolog gene family, member Q | Expression in DCM, correlation with BNP ($r$ = 0.711) | >0.005 | No change | No change | No change |
| 78801_at | *STK38* | Serine/threonine kinase 38 | Kinase activity, correlation with PAP ($r$ = 0.736) | >0.005 | No change | No change | No change |

PAP, pulmonary artery pressure; GPCR, G-protein-coupled receptor; CHF, congestive heart failure; BNP, brain natriuretic peptide; CVD, cardiovascular disease; MI, myocardial infarction; DCM, dilated cardiomyopathy; PA, phenylalanine. *p* value indicates the significance of the difference between the gene expression level of failing and non-failing myocardium.

gene promoted [$^3$H]phenylalanine incorporation; and the overexpression of six genes lowered the viability of cardiomyocytes, which was evaluated by Alamar blue assay. We also evaluated the phenotype of transfected cardiomyocytes. Unlike control cells, *MYLK3*-adenovirus-transfected cardiomyocytes were spike shaped. The overexpression of *GPR37L1* induced apoptosis of cardiomyocytes. The transfection of *NBC1*-adenoviral vectors modified the beating rate of cardiomyocytes (data not shown). Then, we analyzed each gene that encoded a distinct cardiomyocyte phenotype by developing gene-targeted mouse models.

### *In vivo analysis using transgenic and knockout mice*

To study the *in vivo* role of the selected genes, we developed genetically modified mice: three transgenic (Tg) mice for *Mylk3*, *Gpr37l1*, or *Nbc1* and three knockout (KO) mice for *Gpr37l1*, *Gpr35*, or *Mmp23*. We estimated hemodynamic parameters using Miller catheter and the heart weight (HW)/body weight (BW). As shown in Fig. 2A, we found that the blood pressure of *Gpr37l1*-KO mice was significantly higher than that of *Gpr37l1*-Tg mice by 61.7 mmHg ($p < 0.01$). Further, the blood pressure of *Gpr35*-KO mice was higher than that of wild type (WT) littermate by 37.5 mmHg ($p < 0.01$). Overexpression with or knockout of *Mylk3*, *Mmp23*, or *Nbc1* did not result in a significant change in the systolic blood pressure. The HW/BW of *Mylk3*-Tg mice was lower than that of *Mylk3*-WT mice (Fig. 2B). The HW/BW was higher in *Gpr37l1*-KO mice than in *Gpr37l1*-Tg mice. The HW/BW in mice with *Nbc1*, *Gpr35*, or *Mmp23* manipulations did not show any difference. These data showed that modification of *Gpr37l1*, *Gpr35*, or *Mylk3* can produce a distinct cardiovascular phenotype *in vivo*.

## Discussion

The present study identified heart failure-related genes using a novel strategy that was different from the conventional microarray analysis approach. Firstly, we constructed global gene expression profiles to analyze the gene expression in 12 human samples of failing myocardium and two samples of non-failing myocardium. Secondly, we prepared datasets of heart failure-related genes associated with the severity of heart failure; this approach is unique to our study and has not been published before. Thirdly, we selected four genes from these datasets by microarray analysis and a literature-based search. We also included four orphan GPCR genes and four other genes with high expression in the heart as possible drug targets for heart failure treatment. Fourthly, we screened the *in vitro* functions of these 12 genes by achieving adenovirus-mediated overexpression of these genes in rat cardiomyocytes. Finally, we generated gene-targeted mouse models of the five selected genes and screened the *in vivo* functions of these genes. Our novel strategy using a microarray analysis revealed three potential targets, namely, *MYLK3*, *GPR37L1*, and *GPR35* for diagnosing and managing heart failure.

End-stage heart failure caused by a variety of cardiovascular diseases including hypertension, cardiomyopathy, and ischemic heart disease features a common phenotype of reduced cardiac function and dilated cardiac chamber. This result strongly suggested the existence of common genes during the development of heart failure, including the genes encoding natriuretic peptides. To identify novel diagnostic or therapeutic targets for heart failure, such as natriuretic peptides, several microarray analyses of genes expressed in failing myocardium have been performed in the last decade by comparing the gene expression levels between different pairs of samples, such as non-failing versus failing hearts [4–6], failing hearts before versus after placement of left-ventricular assisting device [7,8], hypertrophic versus failing hearts [9], ischemic versus non-ischemic hearts [10]. However, the severity of heart failure is not fixed, but varies from mild to severe heart failure in these studies. To identify the therapeutic targets for heart failure effectively, we believe that it is important to consider the severity of heart failure with microarray data analysis. In this study, we prepared new datasets of heart failure-associated genes that were selected from gene expression profiles of 12 human failing myocardial samples using clinical parameters. A number of genes were associated with PAP, which is an index for the severity of heart failure, whereas only two genes correlated with EF, which is an index for cardiac contractility. This result implies that the stress caused to the heart, and not the ability of cardiac contraction, regulates gene expression in heart failure. We also selected heart failure-related genes whose expression correlated to

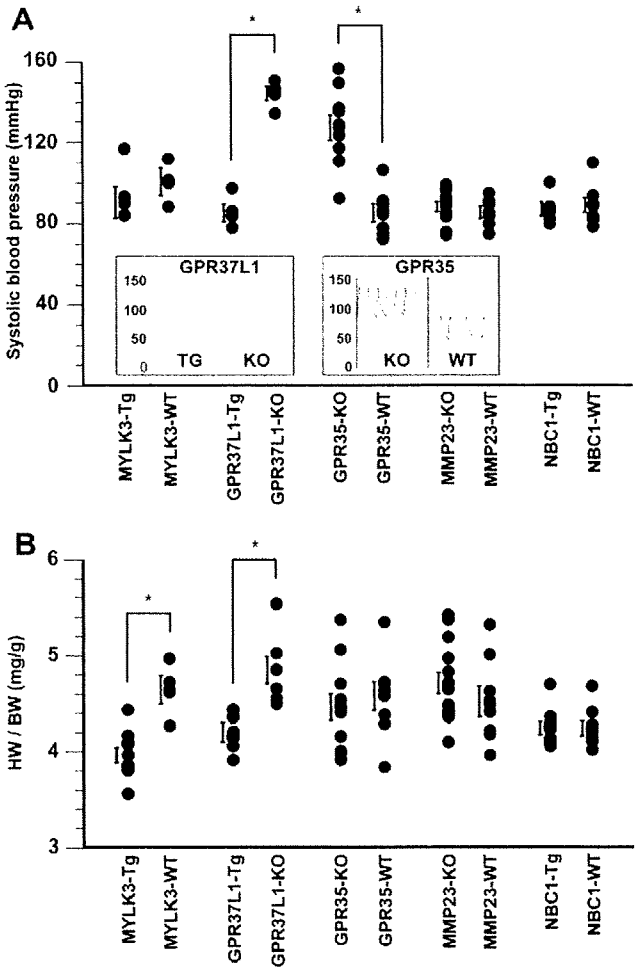


**Fig. 2.** *In vivo* functional analysis using gene-targeting mice of the *Mylk3*, *Gpr37l1*, *Gpr35*, *Mmp23*, and *Nbc1* genes. Blood pressure and heart weight (HW)/body weight (BW) of transgenic (Tg), knockout (KO) and their wild type (WT) littermate mice of each gene were investigated. Values are means ± SEM. $^{*}p < 0.01$. (A) Systolic blood pressure measured using Millar catheter inserted via right carotid artery. The monitoring chart shows representative data of *Gpr37l1*- and *Gpr35*-manipulated mice. (B) HW/BW ratio of each gene-targeting mouse.

the BNP mRNA level, which is the best known indicator of heart failure. The approach used in our study can help in efficient identification of the diagnostic or therapeutic targets for heart failure rather than only comparing two types of samples such as failing versus non-failing myocardium. Among the genes from these new datasets, we focused on the genes exhibiting high expression in heart tissues and finally selected four genes for performing the screening of functional analysis *in vitro*. The expression level of *MYLK3* gene was highly correlated to PAP, and this gene was detected only in the heart tissue. Recently, we reported that *MYLK3* plays a crucial role in sarcomere assembly via phosphorylation of myosin regulatory light chain 2V (MLC2v) [13]. We also showed that the knockdown of *MYLK3* by using a morpholino oligo caused immature sarcomere formation leading to ventricular dilation in zebrafish. These results indicate that *MYLK3* is strongly associated with the pathophysiology of heart failure. Chan et al. also reported that MYLK3 phosphorylates MLC2v and regulates sarcomere organization [15]. These reports affirm the reliability of our original strategy that involves the microarray analysis of failing myocardium. Among these genes, most genes including *XPR1*, *PRDX4*, and *SMOC2* have not been reported to link with cardiovascular phenotypes and were not included in many gene expression profiles published previously.

Next, we performed *in vivo* functional analysis of five selected genes, and we found that gene-targeted mouse models of *Mylk3*, *Gpr37l1*, or *Gpr35* showed the cardiovascular phenotype. As described above, *Mylk3* plays a crucial role in failing heart. In this study, we identified two GPCRs, namely, *Gpr37l1* and *Gpr35*, whose modification affects systolic blood pressure or HW/BW. To our knowledge, this is the first report about the role of these genes in cardiovascular system.

GPCRs constitute one of the largest protein families, but many GPCRs remain to be orphaned. GPR35 is now known to have some ligands such as kynurenic acid (KYNA) [16], zaprinast [17], and 5-nitro-2-(3-phenylpropylamino) benzoic acid [18]. These agonists mobilize intracellular calcium concentration. Therefore, lowering systolic blood pressure in *Gpr35*-KO mice can be induced by modulating calcium release from calcium-storing organelles. Among the three agonists, only KYNA is produced endogenously as a metabolite of tryptophan. Although GPR35 gene expression is supposed to be specific to immune cells and gastrointestinal tract, we found that GPR35 gene expression increased in failing myocardium. In an inflammatory state, interferon γ induces idolemine 2,3-dioxygenase, a rate-limiting enzyme involved in tryptophan degradation, resulting in a substantial increase in KYNA. Inflammation is thought to be involved in the pathogenesis of dilated cardiomyopathy as well as myocardial infarction. Hence there is a possibility that a KYNA-GPR35 signaling plays a role in the pathogenesis of cardiovascular diseases.

Unlike GPR35, GPR37L1 is still orphaned. However, we found that *Gpr37l1*-KO mice showed significant high blood pressure and high HW/BW as compared to Tg mice, which implies the existence of cardiovascular-related function of *Gpr37l1*. Identification of the ligand and the function of this orphan receptor are awaited.

Although no significant phenotype was observed in *Mmp23* and *Nbc1*-Tg mice, we have been investigating their cardiac function in pathological condition such as myocardial infarction or hypertension and determined their detrimental effect on heart failure (data not shown).

In the present study, we determined 12 novel heart failure-related genes by integrating an original method with parameters that indicated disease severity. Further, we assessed these possible targets of drug discovery. *MYLK3*, *GPR37L1*, and *GPR35* were the newly identified targets that play an interesting role in the cardiovascular system.

## Acknowledgments

This study was supported by Grant-in-Aid for Scientific Research (C) in Japan Society for the Promotion of Science; a grant from Human Genome Tissue Engineering and Food Biotechnology in Health and Labor Science Research from the Ministry of Health, Labor, and Welfare, Japan; and a grant from Japan Cardiovascular Research Foundation.

## Appendix A. Supplementary data

Supplementary data associated with this article can be found, in the online version, at doi:10.1016/j.bbrc.2010.01.076.

## References

[1] Effect of enalapril on survival in patients with reduced left ventricular ejection fractions and congestive heart failure. The SOLVD Investigators, N. Engl. J. Med. 325 (1991) 293–302.
[2] Effect of metoprolol CR/XL in chronic heart failure: metoprolol CR/XL randomised intervention trial in congestive heart failure (MERIT-HF), Lancet 353 (1999) 2001–2007.

[3] M. Packer, M.R. Bristow, J.N. Cohn, W.S. Colucci, M.B. Fowler, E.M. Gilbert, N.H. Shusterman, The effect of carvedilol on morbidity and mortality in patients with chronic heart failure. U.S. Carvedilol Heart Failure Study Group, N. Engl. J. Med. 334 (1996) 1349–1355.
[4] J. Yang, C.S. Moravec, M.A. Sussman, N.R. DiPaola, D. Fu, L. Hawthorn, C.A. Mitchell, J.B. Young, G.S. Francis, P.M. McCarthy, M. Bond, Decreased SLIM1 expression and increased gelsolin expression in failing human hearts measured by high-density oligonucleotide arrays, Circulation 102 (2000) 3046–3052.
[5] J.D. Barrans, P.D. Allen, D. Stamatiou, V.J. Dzau, C.C. Liew, Global gene expression profiling of end-stage dilated cardiomyopathy using a human cardiovascular-based cDNA microarray, Am. J. Pathol. 160 (2002) 2035–2043.
[6] F.L. Tan, C.S. Moravec, J. Li, C. Apperson-Hansen, P.M. McCarthy, J.B. Young, M. Bond, The gene expression fingerprint of human heart failure, Proc. Natl. Acad. Sci. USA 99 (2002) 11387–11392.
[7] B.C. Blaxall, B.M. Tschannen-Moran, C.A. Milano, W.J. Koch, Differential gene expression and genomic patient stratification following left ventricular assist device support, J. Am. Coll. Cardiol. 41 (2003) 1096–1106.
[8] J.L. Hall, E.J. Birks, S. Grindle, M.E. Cullen, P.J. Barton, J.E. Rider, S. Lee, S. Harwalker, A. Mariash, N. Adhikari, N.J. Charles, L.E. Felkin, S. Polster, R.S. George, L.W. Miller, M.H. Yacoub, Molecular signature of recovery following combination left ventricular assist device (LVAD) support and pharmacologic therapy, Eur. Heart J. 28 (2007) 613–627.
[9] J. Rysa, H. Leskinen, M. Ilves, H. Ruskoaho, Distinct upregulation of extracellular matrix genes in transition from hypertrophy to hypertensive heart failure, Hypertension 45 (2005) 927–933.
[10] M.M. Kittleson, S.Q. Ye, R.A. Irizarry, K.M. Minhas, G. Edness, J.V. Conte, G. Parmigiani, L.W. Miller, Y. Chen, J.L. Hall, J.G. Garcia, J.M. Hare, Identification of a gene expression profile that differentiates between ischemic and nonischemic cardiomyopathy, Circulation 110 (2004) 3444–3451.
[11] A.S. Barth, R. Kuner, A. Buness, M. Ruschhaupt, S. Merk, L. Zwermann, S. Kaab, E. Kreuzer, G. Steinbeck, U. Mansmann, A. Poustka, M. Nabauer, H. Sultmann, Identification of a common gene expression signature in dilated cardiomyopathy across independent microarray studies, J. Am. Coll. Cardiol. 48 (2006) 1610–1617.
[12] M. Asakura, M. Kitakaze, Global gene expression profiling in the failing myocardium, Circ. J. 73 (2009) 1568–1576.
[13] O. Seguchi, S. Takashima, S. Yamazaki, M. Asakura, Y. Asano, Y. Shintani, M. Wakeno, T. Minamino, H. Kondo, H. Furukawa, K. Nakamaru, A. Naito, T. Takahashi, T. Ohtsuka, K. Kawakami, T. Isomura, S. Kitamura, H. Tomoike, N. Mochizuki, M. Kitakaze, A cardiac myosin light chain kinase regulates sarcomere assembly in the vertebrate heart, J. Clin. Invest. 117 (2007) 2812–2824.
[14] M. Asakura, M. Kitakaze, S. Takashima, Y. Liao, F. Ishikura, T. Yoshinaka, H. Ohmoto, K. Node, K. Yoshino, H. Ishiguro, H. Asanuma, S. Sanada, Y. Matsumura, H. Takeda, S. Beppu, M. Tada, M. Hori, S. Higashiyama, Cardiac hypertrophy is inhibited by antagonism of ADAM12 processing of HB-EGF: metalloproteinase inhibitors as a new therapy, Nat. Med. 8 (2002) 35–40.
[15] J.Y. Chan, M. Takeda, L.E. Briggs, M.L. Graham, J.T. Lu, N. Horikoshi, E.O. Weinberg, H. Aoki, N. Sato, K.R. Chien, H. Kasahara, Identification of cardiac-specific myosin light chain kinase, Circ. Res. 102 (2008) 571–580.
[16] J. Wang, N. Simonavicius, X. Wu, G. Swaminath, J. Reagan, H. Tian, L. Ling, Kynurenic acid as a ligand for orphan G protein-coupled receptor GPR35, J. Biol. Chem. 281 (2006) 22021–22028.
[17] Y. Taniguchi, H. Tonai-Kachi, K. Shinjo, Zaprinast, a well-known cyclic guanosine monophosphate-specific phosphodiesterase inhibitor, is an agonist for GPR35, FEBS Lett. 580 (2006) 5003–5008.
[18] Y. Taniguchi, H. Tonai-Kachi, K. Shinjo, 5-Nitro-2-(3-phenylpropylamino)-benzoic acid is a GPR35 agonist, Pharmacology 82 (2008) 245–249.

Journal of the American College of Cardiology
© 2009 by the American College of Cardiology Foundation
Published by Elsevier Inc.

Vol. 53, No. 22, 2009
ISSN 0735-1097/09/$36.00
doi:10.1016/j.jacc.2009.02.038



# Natriuretic Peptides Enhance the Production of Adiponectin in Human Adipocytes and in Patients With Chronic Heart Failure

Osamu Tsukamoto, MD, PHD,*‡ Masashi Fujita, MD, PHD,‡ Mahoto Kato, MD,* Satoru Yamazaki, PHD,* Yoshihiro Asano, MD, PHD,‡ Akiko Ogai, PHD,* Hidetoshi Okazaki, MD, PHD,* Mitsutoshi Asai, MD,‡ Yoko Nagamachi, BS,‡ Norikazu Maeda, MD, PHD,§ Yasunori Shintani, MD, PHD,‡ Tetsuo Minamino, MD, PHD,‡ Masanori Asakura, MD, PHD,* Ichiro Kishimoto, MD, PHD,† Tohru Funahashi, MD, PHD,§ Hitonobu Tomoike, MD, PHD,* Masafumi Kitakaze, MD, PHD*

*Suita, Osaka, Japan*

**Objectives** We investigated the functional relationship between natriuretic peptides and adiponectin by performing both experimental and clinical studies.

**Background** Natriuretic peptides are promising candidates for the treatment of congestive heart failure (CHF) because of their wide range of beneficial effects on the cardiovascular system. Adiponectin is a cytokine derived from adipose tissue with various cardiovascular-protective effects that has been reported to show a positive association with plasma brain natriuretic peptide (BNP) levels in patients with heart failure.

**Methods** The expression of adiponectin messenger ribonucleic acid (mRNA) and its secretion were examined after atrial natriuretic peptide (ANP) or BNP was added to primary cultures of human adipocytes in the presence or absence of HS142-1 (a functional type A guanylyl cyclase receptor antagonist). Changes of the plasma adiponectin level were determined in 30 patients with CHF who were randomized to receive intravenous ANP (0.025 μg/kg/min human ANP for 3 days, n = 15) or saline (n = 15).

**Results** Both ANP and BNP dose-dependently enhanced the expression of adiponectin mRNA and its secretion, whereas such enhancement was inhibited by pre-treatment with HS142-1. The plasma adiponectin level was increased at 4 days after administration of human ANP compared with the baseline value (from 6.56 ± 0.40 μg/ml to 7.34 ± 0.47 μg/ml, $p < 0.05$), whereas there was no change of adiponectin in the saline group (from 6.53 ± 0.57 μg/ml to 6.55 ± 0.56 μg/ml).

**Conclusions** Natriuretic peptides enhance adiponectin production by human adipocytes in vitro and even in patients with CHF, which might have a beneficial effect on cardiomyocytes in patients receiving recombinant natriuretic peptide therapy for heart failure. (J Am Coll Cardiol 2009;53:2070–7) © 2009 by the American College of Cardiology Foundation

Plasma natriuretic peptide levels are increased in patients with congestive heart failure (CHF), and the measurement of these peptides is used widely to assess the presence, severity, and prognosis of CHF (1,2). Both atrial natriuretic peptide and brain natriuretic peptide (ANP and BNP, respectively) have a beneficial effect in patients with heart failure because of their various biological actions (3–5).

See page 2078

Adiponectin is a circulating cytokine derived from adipose tissue that has attracted considerable interest because of its identification as a risk factor for cardiovascular disease (6,7) and CHF (8). Adiponectin production is downregulated in patients with coronary risk factors that are associated with the development of heart failure (9,10).

From the Cardiovascular Division of *Medicine and †Biochemistry, National Cardiovascular Center, Suita, Osaka, Japan; and the Departments of ‡Cardiovascular Medicine and §Metabolic Medicine, Osaka University Graduate School of Medicine, Suita, Osaka, Japan. This work is supported by grants-in-aid from the Ministry of Health, Labor, and Welfare-Japan, grants-in-aid from the Ministry of Education, Culture, Sports, Science and Technology-Japan, grants from the Japan Heart Foundation, and grants from the Japan Cardiovascular Research Foundation (all to Dr. Kitakaze) and Takeda Medical Research Foundation (to Dr. Funahashi). Drs. Tsukamoto, Fujita, and Kato contributed equally to this work.

Manuscript received August 27, 2008; revised manuscript received January 22, 2009, accepted February 19, 2009.

Recently, adiponectin was reported to have a cardioprotective effect against ischemia-reperfusion injury (11) and hemodynamic stress (12,13) in mice. Interestingly, it has been reported that the level of N-terminal pro-brain natriuretic peptide shows a positive correlation with the plasma adiponectin concentration in patients with chronic heart failure (14).

Given these experimental and clinical observations, we hypothesized that natriuretic peptides might increase adiponectin production in patients with heart failure to protect the cardiovascular system. Accordingly, in the present study, we investigated whether natriuretic peptides could directly increase adiponectin production by these adipocytes (and the cellular mechanisms involved) and confirmed this effect on adiponectin in the clinical setting.

**Abbreviations and Acronyms**

ANP = atrial natriuretic peptide
BNP = brain natriuretic peptide
CHF = congestive heart failure
GC-A = type A guanylyl cyclase receptor
hANP = human atrial natriuretic peptide
NPR = natriuretic peptide receptor
PKG = protein kinase G

## Methods

**Agents.** Both human ANP and BNP were purchased from Sigma-Aldrich (St. Louis, Missouri). HS142-1, a functional guanylyl cyclase-A type receptor antagonist, was provided by Kyowa Hakko Kogyo Co., Ltd. (Mishima, Japan). A cGMP analog (8-pCPT-cGMP) and a selective cGMP-dependent protein kinase G (PKG) inhibitor ($R_p$-8-Br-PET-cGMP-S) were obtained from Biolog Life Science Institute (Bremen, Germany). An antibody directed against mouse adiponectin (MAB3608) was purchased from Chemicon International, Inc.

**Primary culture and in vitro study of human adipocytes.** Subcutaneous adipocytes derived from the adipose tissue of 6 women were obtained commercially together with culture medium from Zen-Bio, Inc. (Research Triangle Park, North Carolina. The donors were nonsmokers with a mean body mass index of 27.0 kg/m$^2$ (range 25.9 to 29.1 kg/m$^2$) and an average age of 47 years (range 29 to 63 years). Cells were maintained in adipocytes maintenance medium (i.e., AM-1) containing Dulbecco's modified Eagle medium/Ham's F-12 (1:1, v/v), 3% fetal calf serum, 15 mmol/l HEPES (pH 7.4), biotin, pantothenate, human insulin, 1 μmol/l dexamethasone, 100 U/ml penicillin, 100 μg/ml streptomycin, and 0.25 μg/ml amphotericin B at 37°C in a humidified atmosphere of 95% air/5% $CO_2$. The medium was changed every 2 days. Primary cultures of the adipocytes were used to examine the effects of natriuretic peptides (ANP or BNP) on the expression of adiponectin.

Before these experiments, the cells were plated in adipocyte basal medium (i.e., BM-1) containing Dulbecco's modified Eagle medium/Ham's F-12 (1:1, volume/volume), 15 mmol/l 4-(2-hydroxyethyl)-1-piperazineethanesulfonic acid (pH 7.4), biotin, and pantothenate for 24 h. Then the indicated concentrations of either natriuretic peptide (from $10^{-11}$ to $10^{-9}$ mol/l) were added to the BM-1 medium. After 24 h of incubation, the medium was harvested for Western blotting to measure the secretion of adiponectin, and the cells were also harvested for ribonucleic acid (RNA) analysis. The effect of each natriuretic peptide on adiponectin messenger ribonucleic acid (mRNA) levels was determined by quantitative real-time polymerase chain reaction (PCR).

**Measurement of adiponectin.** In patients with CHF, the plasma adiponectin concentration was measured by the use of an ELISA kit (Otsuka Pharmaceutical Co., Ltd., Tokyo, Japan) according to the manufacturer's protocol. Adiponectin secretion by primary cultured human adipocytes was assessed by Western blotting of the culture medium, as previously described (15), and the immunoreactive bands were quantified by densitometry (Molecular Dynamics, Sunnyvale, California).

**Reverse transcriptional-PCR.** Total RNA was extracted from adipocytes derived from human white fat with the use of RNA-Bee-RNA Isolation Reagent (Tel-Test, Inc., Gainesville, Florida). Then, 200 ng of total RNA was reversed transcribed and amplified by the use of an Omniscript RT kit (Qiagen, Hilden, Germany) according to the manufacturer's protocol. The forward primers for type A guanylyl cyclase receptor (GC-A) and natriuretic peptide receptor (NPR)-C were 5′-CCAGTTCCAAGTCTTTGCCAAGACAGCA and 5′-GGAAGACATCGTGCGCAATA, respectively, and the reverse primers for GC-A and NPR-C were 5′-CATTGTGTAGAAACAGCATGCCCTTGACGA and 5′-TGCTCCGGATGGTGTCACT, respectively. As a positive control, we used the samples of human cardiac tissue under the protocol approved by the institutional review board of the National Cardiovascular Center (No. 14-18) (16).

**Quantitative real-time PCR analysis.** Quantitative real-time PCR was performed as described previously (17). Oligonucleotide primers and TaqMan probes for human adiponectin and glyceraldehyde 3-phosphate dehydrogenase were purchased from Applied Biosystems (Foster City, California).

**Subjects and design of the clinical study.** We prospectively studied 30 consecutive CHF patients who were admitted to the emergency department of the National Cardiovascular Center between April and July 2006. The exclusion criteria were as follows: age >80 years, cardiogenic shock or hypotension (systolic blood pressure <100 mm Hg), and renal failure (serum creatinine >2.0 mg/dl). This study was approved by the Committee on Human Investigation of the National Cardiovascular Center, and all patients who participated gave informed consent. The 30 patients were randomized to 2 groups, a human atrial natriuretic peptide (hANP) group consisting of 15 patients who received administration of hANP and a control group consisting of 15 patients who were administered saline. In the hANP group, from immediately after the diagnosis of

acute exacerbation of CHF, hANP (0.025 μg/kg/min) was infused intravenously for 3 days. The study protocol did not restrict or specify any other diagnostic or therapeutic strategies. Blood for measuring the plasma adiponectin level was sampled before and 1 and 7 days after finishing the administration of hANP or saline (days 1, 4, and 10, respectively) (Fig. 3A).

**Statistical analysis.** For analysis of differences between the various treatments of adipocytes, analysis of variance was performed, followed by the appropriate post-hoc test. The differences in adiponectin levels between days 1 and 4 in each group were tested with a paired *t* test. The changes in adiponectin levels from day 1 to 4 between ANP group and saline group was tested with an unpaired *t* test. Results are expressed as the mean ± SEM, and p values of $<0.05$ were considered significant.

## Results

**Effect of natriuretic peptides on the expression and secretion of adiponectin by primary cultured human adipocytes.** First, we checked the expression of GC-A and NPR-C mRNA by using reverse transcriptional-PCR. As shown in Figure 1A, both GC-A and NPR-C mRNA was detectable in primary cultured human adipocytes. To investigate the effects of natriuretic peptides on the regulation of adiponectin production in adipocytes, we incubated primary cultured human adipocytes with recombinant ANP. When ANP was used at a concentration of $10^{-10}$ mol/l (pathological plasma concentration), it increased adiponectin mRNA expression after 6 h of incubation and reached a maximum after 12 h (Fig. 1B). Next, we incubated human adipocytes with ANP at the concentration of from $10^{-11}$ mol/l (normal plasma concentration) to $10^{-9}$ mol/l (pharmacological plasma concentrations) and demonstrated enhanced adiponectin mRNA expression and adiponectin secretion into the medium in a dose-dependent manner, whereas these changes were completely inhibited by pretreatment with HS142-1 (Figs. 1C and 1D). Incubation of adipocytes with BNP also increased the expression of adiponectin mRNA in a dose-dependent manner and this effect was completely blocked by pretreatment with HS142-1 (Figs. 1E and 1F).

**Involvement of cGMP/PKG signaling in natriuretic peptide-induced synthesis of adiponectin.** Because both ANP and BNP exert their biological effects by promoting cGMP production, to investigate the role of the GC-A/cGMP/PKG signaling pathway in adiponectin production, we measured the changes of cGMP in ANP-treated primary cultured human adipocytes. We found that incubation with ANP increased the cGMP level and that this effect was blunted by co-treatment with HS142-1 (data not shown). Next, we treated human adipocytes with the cGMP analog 8-pCPT-cGMP and the PKG inhibitor ($R_p$)-8-Br-PET-cGMP-S. The activation of PKG by 8-pCPT-cGMP (50 μmol/l for 12 h) produced an increase of adiponectin mRNA expression similar to that observed after incubation with ANP. The effect of ANP on adiponectin mRNA expression was abolished in the presence of ($R_p$)-8-Br-PET-cGMP-S (100 nmol/l) (Fig. 2A). Consistent with these findings, adiponectin secretion into the culture medium also was increased by stimulation of the cGMP/PKG-dependent pathway (Fig. 2B). These results suggested that natriuretic peptides promote adiponectin synthesis via the GC-A/cGMP/PKG-dependent pathway.

**Increase of plasma adiponectin levels in CHF patients treated with hANP.** To confirm the effect of natriuretic peptides on the production of adiponectin, we conducted the clinical study. Thirty consecutive patients who met the inclusion criteria were enrolled in this clinical study. Fifteen patients were randomized to the ANP group, and 15 were assigned to the saline group. Baseline variables and treatments of the 2 groups are shown in Table 1. There were no differences in baseline clinical characteristics, hemodynamics, biochemical data, or medications. There was also no significant difference in the baseline plasma level of adiponectin between the 2 groups. As shown in Figure 3B, the plasma level of adiponectin did not change throughout the study in the saline group. On the other hand, the plasma adiponectin level at 1 day after finishing the administration of hANP (day 4) was significantly increased compared with the baseline value (day 1) in the ANP group, and it returned to baseline by 7 days after the completion of hANP infusion (day 10). These results suggested that hANP infusion led to an increase of the plasma adiponectin level in patients with CHF.

## Discussion

In the present study, we demonstrated a novel effect of natriuretic peptides (ANP and BNP) on the production of adiponectin by adipocytes in both experimental and clinical studies. First, we clearly demonstrated that pathophysiological and pharmacological concentrations of either ANP or BNP increased adiponectin synthesis by primary cultured human adipocytes. Second, we showed that administration of recombinant ANP increased the plasma adiponectin level in patients with CHF.

ANP and BNP play an important role in the regulation of cardiovascular homeostasis. Their actions are primarily mediated via GC-A, which is expressed in various tissues and organs, including the kidneys, blood vessels, adrenal glands, and heart (18). Consistent with a previous report (19), we demonstrated that GC-A and NPR-C are expressed by human adipocytes. In the present study, we demonstrated a novel effect of both ANP and BNP on primary cultured human adipocytes, which was that pathophysiological or pharmacological concentrations of both peptides augmented adiponectin production by human adipocytes, with this effect being inhibited by treatment with HS142-1. Furthermore, we demonstrated that natriuretic peptides augment the production of adiponectin via a cGMP-dependent

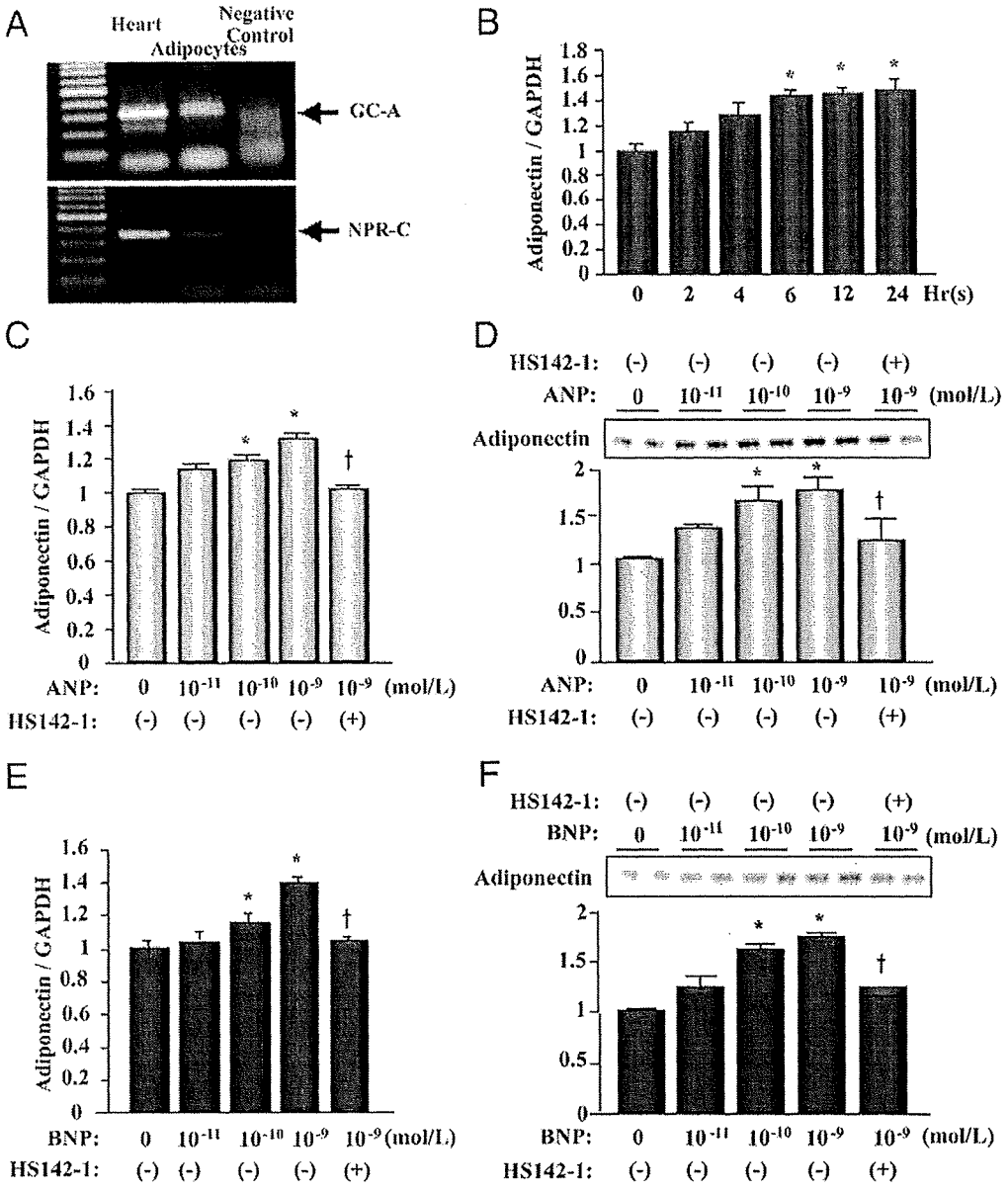


**Figure 1** **Effect of Natriuretic Peptides on the Expression and Secretion of Adiponectin by Primary Human Adipocytes**

**(A)** Expression of GC-A receptors **(top)** and NPR-C **(bottom)** mRNA by primary cultured human adipocytes. Reverse-transcription PCR revealed expression of both GC-A receptors and NPR-C by human adipocytes. **(B)** Effect of ANP ($10^{-10}$ mol/l) on the expression of adiponectin mRNA as determined by quantitative real-time PCR. **(C)** Dose-dependent effect of ANP on adiponectin mRNA expression, as determined by quantitative real-time PCR. Human adipocytes were treated with the indicated concentrations of ANP for 24 h. **(D)** Dose-dependent effect of ANP on adiponectin secretion into the culture medium. **(Top)** A representative Western blot of adiponectin. **(Bottom)** Quantitative analysis of adiponectin by densitometry. Values are normalized to the control. *$p < 0.05$ versus control, †$p < 0.05$ versus ANP $10^{-9}$ mol/l. **(E)** Dose-dependent effect of BNP on adiponectin mRNA expression, as determined by quantitative real-time PCR. **(F)** Dose-dependent effect of BNP on adiponectin secretion into the culture medium as determined by Western blotting. **(Top)** Representative Western blot of adiponectin. **(Bottom)** Quantitative analysis of adiponectin by densitometry. Values are normalized to the control. *$p < 0.05$ versus control. †$p < 0.05$ versus BNP $10^{-9}$ mol/l. ANP = atrial natriuretic peptide; BNP = brain natriuretic peptide; GC-A = type A guanylyl cyclase receptor; mRNA = messenger ribonucleic acid; NPR-C = natriuretic peptide receptor C; PCR = polymerase chain reaction.

pathway. These findings are important evidence that ANP and BNP regulate adiponectin production by human adipocytes.

Intravenous infusion of nesiritide (recombinant human BNP) has been reported to have beneficial hemodynamic effects in patients with CHF (4,5). The use of ANP also has been reported to have beneficial effects in patients with acute myocardial infarction (20,21). These beneficial effects have been attributed to the cardiovascular-protective actions of natriuretic peptides, including diuresis, natriuresis, vaso-

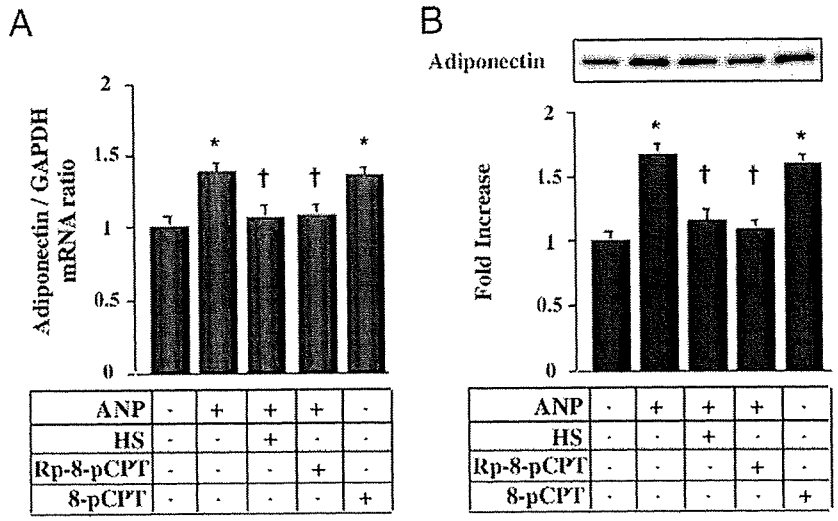


**Figure 2** Involvement of the cGMP/PKG Signaling Pathway in the Induction of Adiponectin Synthesis by ANP

**(A, B)** Involvement of PKG was assessed by the treatment of primary cultured human adipocytes with 8-pCPT-cGMP (8-pCPT) and ($R_p$)-8-Br-PET-cGMP-S (Rp-8-pCPT). Adiponectin mRNA levels were determined by quantitative real-time PCR **(A)** and secretion of adiponectin into the culture medium was determined by Western blotting. Quantitative analysis of adiponectin secretion into the culture medium was done by densitometry **(B)**. Values are normalized to the control. *p < 0.05 versus control. †p < 0.05 versus ANP. HS = HS142-1; other abbreviations as in Figure 1.

dilation, and reduction of activity of the sympathetic nervous system and the renin-angiotensin-aldosterone system (3–5). In the present study, we administered recombinant ANP to patients with CHF and observed the changes of plasma adiponectin. The plasma adiponectin level of the ANP group was increased at 1 day after the finish of ANP administration compared with that in the control group, and then returned to baseline by 7 days after the completion of administration in patients with CHF.

Importantly, Moro et al. (22) showed that ANP did not affect the secretion of adiponectin in human abdominal adipose tissue from overweight women. This result may appear contradict ours, but we believe that is not the case. First, the concentration of ANP they used ($10^{-6}$ mol/l) in the experiment of cultured adipocytes was greater than our concentration. Second, our data that recombinant ANP increased the plasma adiponectin levels were drawn from patients with heart failure, whereas the data of Moro et al. (22) were from cultured fat tissues of overweight women who underwent plastic surgery. However, they also demonstrated the potential stimulatory effect of ANP on adiponectin production from human adipose tissue in the presence of

**Table 1** Clinical Characteristics of the 2 Groups

| | hANP Group (n = 15) | Saline Group (n = 15) | p Value |
|---|---|---|---|
| Age (yrs) | 60 ± 19 | 59 ± 19 | NS |
| Sex (male/female) | 9/6 | 10/5 | NS |
| Heart rate (beats/min) | 62 ± 11 | 66 ± 7 | NS |
| Body mass index (kg/m$^2$) | 21.4 ± 1.1 | 21.1 ± 1.7 | NS |
| Systolic blood pressure (mm Hg) | 116 ± 9 | 113 ± 9 | NS |
| Diastolic blood pressure (mm Hg) | 76 ± 12 | 74 ± 6 | NS |
| NYHA functional class (II/III) | 14/1 | 10/5 | NS |
| LVEF by echocardiography (%) | 32 ± 2 | 31 ± 8 | NS |
| Plasma BNP (pg/ml) | 506 ± 39 | 537 ± 33 | NS |
| Other medications n (%) | | | |
| Loop diuretics | 9 (60) | 10 (67) | NS |
| Spironolactone | 5 (33) | 8 (53) | NS |
| ACEI or ARB | 12 (80) | 11 (80) | NS |
| Beta-blockers | 13 (86) | 12 (80) | NS |

ACEI = angiotensin-converting enzyme inhibitors; ARB = angiotensin II receptor blockers; BNP = brain natriuretic peptide; hANP = human atrial natriuretic peptide; LVEF = left ventricular ejection fraction; NS = not significant; NYHA = New York Heart Association.

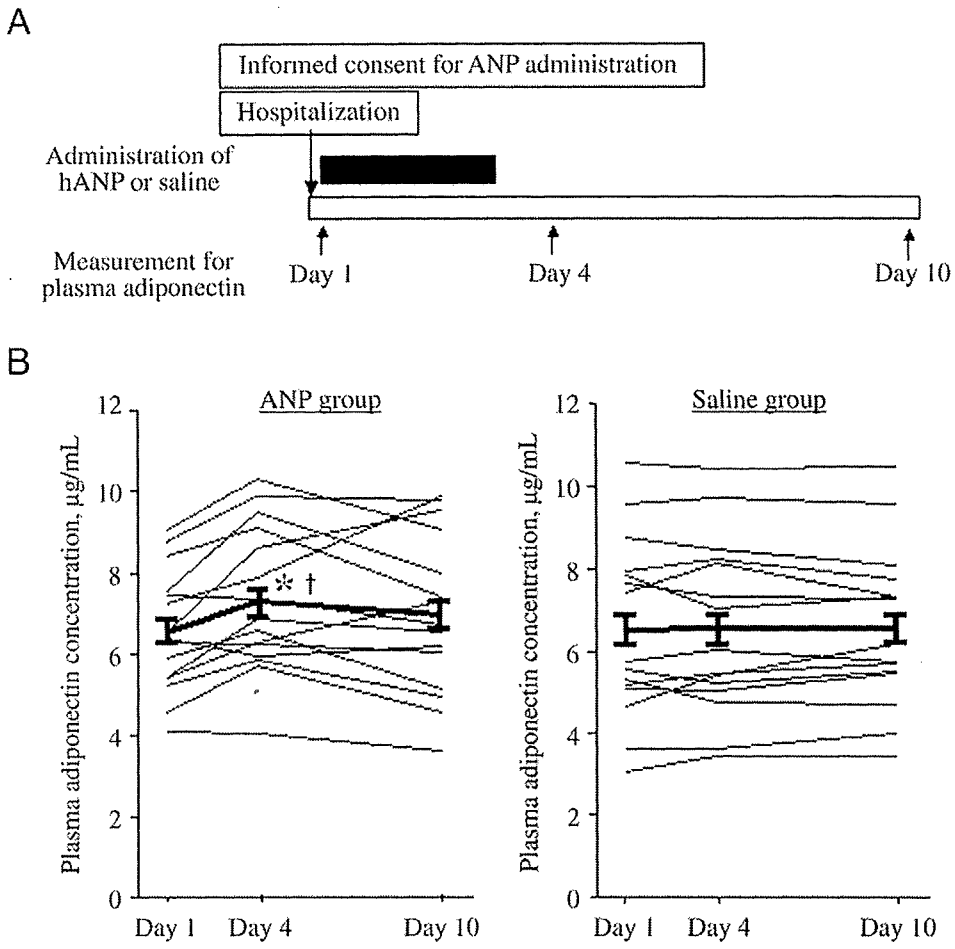


**Figure 3** **Increased Plasma Adiponectin Level in Patients With CHF After ANP Treatment**

**(A)** Outline of the study protocol. hANP or saline was infused continuously for 3 days in the ANP and saline groups, respectively. The **black bar** indicates administration of either hANP (0.025 μg/kg/min) or saline. **(B)** The plasma adiponectin concentration profile after treatment in both groups. *$p < 0.05$ versus baseline in the ANP group; †$p < 0.05$ versus at the corresponding time in the saline group. CHF = congestive heart failure; hANP = human atrial natriuretic peptide; other abbreviations as in Figure 1.

hormone-sensitive lipase inhibitor, which inhibits the formation of lipolysis-derived byproducts by ANP-induced lipolysis (22).

Recently, Yu et al. (23) demonstrated the increased ANP-induced lipolysis rates in large adipocytes compared with small adipocytes. Thus, the difference of adipocyte size between patients with CHF and obesity might contribute to the different pattern of adiponectin secretion. Finally, catecholamines also are involved in the control of lipolysis in humans (24). Thus, the prolonged exposure of high plasma level of catecholamines or the treatment with beta-adrenergic receptor blockers in patients with CHF also might affect the distinct pattern of adiponectin secretion from adipocytes. Although precise mechanisms are unknown, the human adipocytes could secrete adiponectin when the certain stress was loaded. However, it remains possible that factors such as tumor necrosis factor-alpha (25) and alpha-adrenergic stimulation (26), both of which are increased in patients with CHF, may influence the expression of adiponectin or that adiponectin levels are affected by medical treatment, so further investigations are needed.

It is not clear whether ANP augments the plasma adiponectin levels in healthy subjects because of the ethical problems. However, we have reported that the plasma adiponectin level increased along with an increase of plasma BNP levels in 1,538 healthy subjects (27). These results suggest that an increase of natriuretic peptides augments the plasma adiponectin levels and exerts a cardioprotective effect in clinical settings.

Under normal conditions the adult heart utilizes predominantly fatty acids to derive the majority of its energy (28). However, metabolic remodeling such as a marked shift in substrate preference away from fatty acids toward glucose is observed in hypertrophic and failing hearts and the decrease

in fatty acid oxidation is not fully compensated for by an increase in glucose oxidation (29). Thus, the failing heart suffers from chronic energy starvation (30). Insulin resistance also is common in patients with heart failure (31). Adiponectin improves both glucose metabolism and insulin resistance via the AMPK signaling pathway (32). Therefore, we believe that the administration of recombinant natriuretic peptide has beneficial effects on cardiac energy metabolism via adiponectin in patients with CHF.

Interestingly, the plasma adiponectin level was reported to be decreased in patients with risk factors for heart failure (9,33–35) and increased along with BNP after the onset of heart failure (14). Although approximately 10% increase in adiponectin levels in the ANP group seems relatively small, this would not be the case because there was about a 20% reduction in plasma adiponectin levels in patients with coronary artery disease compared with those in control subjects (35), which leads us to believe that the 10% increase in adiponectin is important from the viewpoint of pathophysiology of heart diseases. Therefore, we hypothesized that ANP and/or BNP regulates the plasma level of adiponectin in patients with CHF and conducted this study.

## Conclusions

We demonstrated that natriuretic peptides increase the production of adiponectin by human adipocytes, as well as in patients with CHF. These findings may help to shed more light on the pathophysiology of heart failure.

### Acknowledgments

The authors thank Yukari Arino and Kieko Segawa for their secretarial work and Maki Miyoshi and Yoko Motomura for their excellent technical assistance.

**Reprint requests and correspondence:** Dr. Masafumi Kitakaze, Department of Cardiovascular Medicine, National Cardiovascular Center, Suita, Osaka 565-8565, Japan. E-mail: kitakaze@zf6.so-net.ne.jp.

### REFERENCES

1. Maisel AS, Krishnaswamy P, Nowak RM, et al. Rapid measurement of B-type natriuretic peptide in the emergency diagnosis of heart failure. N Engl J Med 2002;347:161–7.
2. Stanek B, Frey B, Hulsmann M, et al. Prognostic evaluation of neurohumoral plasma levels before and during beta-blocker therapy in advanced left ventricular dysfunction. J Am Coll Cardiol 2001;38:436–42.
3. Levin ER, Gardner DG, Samson WK. Natriuretic peptides. N Engl J Med 1998;339:321–8.
4. Mills RM, LeJemtel TH, Horton DP, et al. Sustained hemodynamic effects of an infusion of nesiritide (human b-type natriuretic peptide) in heart failure: a randomized, double-blind, placebo-controlled clinical trial. Natrecor Study Group. J Am Coll Cardiol 1999;34:155–62.
5. Colucci WS, Elkayam U, Horton DP, et al. Intravenous nesiritide, a natriuretic peptide, in the treatment of decompensated congestive heart failure. Nesiritide Study Group. N Engl J Med 2000;343:246–53.
6. Lakka HM, Laaksonen DE, Lakka TA, et al. The metabolic syndrome and total and cardiovascular disease mortality in middle-aged men. JAMA 2002;288:2709–16.
7. Ninomiya JK, L'Italien G, Criqui MH, Whyte JL, Gamst A, Chen RS. Association of the metabolic syndrome with history of myocardial infarction and stroke in the Third National Health and Nutrition Examination Survey. Circulation 2004;109:42–6.
8. Ingelsson E, Sundstrom J, Arnlov J, Zethelius B, Lind L. Insulin resistance and risk of congestive heart failure. JAMA 2005;294:334–41.
9. Kenchaiah S, Evans JC, Levy D, et al. Obesity and the risk of heart failure. N Engl J Med 2002;347:305–13.
10. Hunt SA, Baker DW, Chin MH, et al. ACC/AHA guidelines for the evaluation and management of chronic heart failure in the adult: executive summary: a report of the American College of Cardiology/American Heart Association Task Force on Practice Guidelines (Committee to Revise the 1995 Guidelines for the Evaluation and Management of Heart Failure). J Am Coll Cardiol 2001;38:2101–13.
11. Shibata R, Sato K, Pimentel DR, et al. Adiponectin protects against myocardial ischemia-reperfusion injury through AMPK- and COX-2-dependent mechanisms. Nat Med 2005;11:1096–103.
12. Shibata R, Ouchi N, Ito M, et al. Adiponectin-mediated modulation of hypertrophic signals in the heart. Nat Med 2004;10:1384–9.
13. Liao Y, Takashima S, Maeda N, et al. Exacerbation of heart failure in adiponectin-deficient mice due to impaired regulation of AMPK and glucose metabolism. Cardiovasc Res 2005;67:705–13.
14. Kistorp C, Faber J, Galatius S, et al. Plasma adiponectin, body mass index, and mortality in patients with chronic heart failure. Circulation 2005;112:1756–62.
15. Maeda N, Takahashi M, Funahashi T, et al. PPARgamma ligands increase expression and plasma concentrations of adiponectin, an adipose-derived protein. Diabetes 2001;50:2094–9.
16. Okada K, Minamino T, Tsukamoto Y, et al. Prolonged endoplasmic reticulum stress in hypertrophic and failing heart after aortic constriction: possible contribution of endoplasmic reticulum stress to cardiac myocyte apoptosis. Circulation 2004;110:705–12.
17. Tsukamoto O, Minamino T, Okada K, et al. Depression of proteasome activities during the progression of cardiac dysfunction in pressure-overloaded heart of mice. Biochem Biophys Res Commun 2006;340:1125–33.
18. Nakao K, Ogawa Y, Suga S, Imura H. Molecular biology and biochemistry of the natriuretic peptide system. II: Natriuretic peptide receptors. J Hypertens 1992;10:1111–4.
19. Sengenes C, Zakaroff-Girard A, Moulin A, et al. Natriuretic peptide-dependent lipolysis in fat cells is a primate specificity. Am J Physiol Regul Integr Comp Physiol 2002;283:R257–65.
20. Kitakaze M, Asakura M, Kim J, et al. Human atrial natriuretic peptide and nicorandil as adjuncts to reperfusion treatment for acute myocardial infarction (J-WIND): two randomised trials. Lancet 2007;370:1483–93.
21. Hayashi M, Tsutamoto T, Wada A, et al. Intravenous atrial natriuretic peptide prevents left ventricular remodeling in patients with first anterior acute myocardial infarction. J Am Coll Cardiol 2001;37:1820–6.
22. Moro C, Klimcakova E, Lolmede K, et al. Atrial natriuretic peptide inhibits the production of adipokines and cytokines linked to inflammation and insulin resistance in human subcutaneous adipose tissue. Diabetologia 2007;50:1038–47.
23. Yu J, Yu HC, Kim KA, et al. Differences in the amount of lipolysis induced by atrial natriuretic peptide in small and large adipocytes. J Pept Sci 2008;14:972–7.
24. Moro C, Galitzky J, Sengenes C, Crampes F, Lafontan M, Berlan M. Functional and pharmacological characterization of the natriuretic peptide-dependent lipolytic pathway in human fat cells. J Pharmacol Exp Ther 2004;308:984–92.
25. Maeda N, Shimomura I, Kishida K, et al. Diet-induced insulin resistance in mice lacking adiponectin/ACRP30. Nat Med 2002;8:731–7.
26. Fasshauer M, Klein J, Neumann S, Eszlinger M, Paschke R. Adiponectin gene expression is inhibited by beta-adrenergic stimulation via protein kinase A in 3T3-L1 adipocytes. FEBS Lett 2001;507:142–6.